Stony Brook University | The State University of New York

Flow and its fluctuations at ATLAS --in large systems

Jiangyong Jia

Stony Brook University and BNL

India+ lectures on Heavy Ion Collision experiments

Outline

- Introduction and flow observables
- ATLAS detector and trigger
- Selected results with analysis details
  - v_n from event plane and two-particle correlation methods
  - Event plane correlations
  - $p(v_n)$ distributions
  - v_n-v_m correlation via event-shape engineering
  - Longitudinal flow decorrelations
- Outlook

High-energy heavy ion collision

$$\frac{\sqrt{s_{\mathrm{NN}}}}{2} = 100 - 2500\ \mathrm{GeV}$$

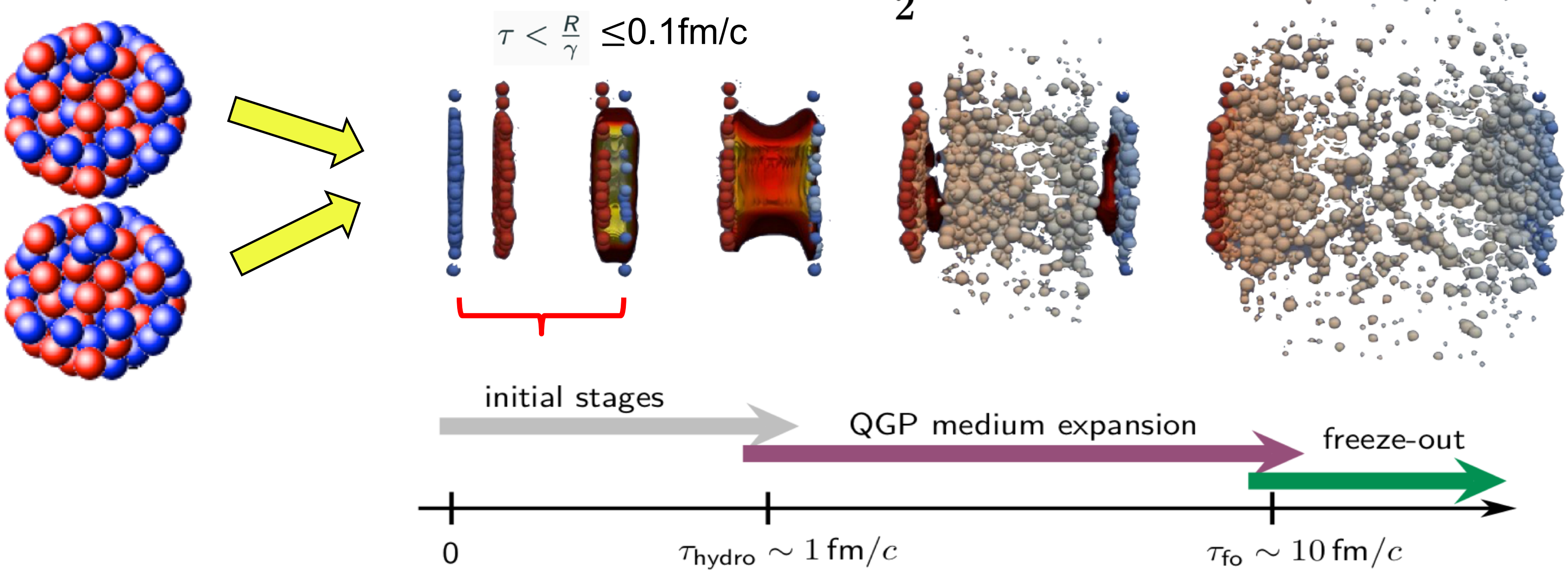

400 nucleons → 30000 hadrons

in 10^{-23} seconds

- Collision takes a snapshot of the nuclear and nucleon wavefunction.
- Large particle production enable description of QGP in terms of hydrodynamics.
- Big unknown: What is the nature of initial condition and pre-equilibrium phase?
- How to probe the dynamics and properties via flow and its fluctuations?

Not covered: small systems, high p_T, heavy flavor, Jet tagged

https://twiki.cern.ch/twiki/bin/view/AtlasPublic/HeavyIonsPublicResults

Connecting the initial and final state

Initial state

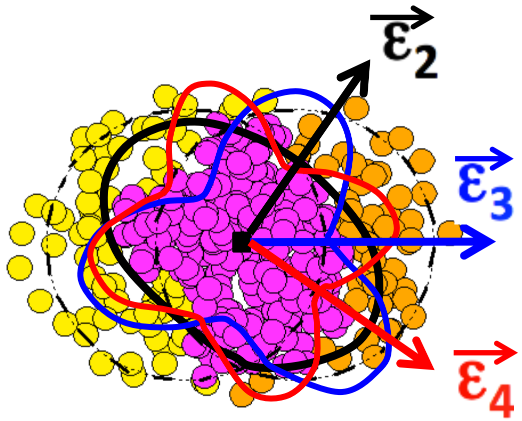

$$\vec{\epsilon}_n \equiv \epsilon_n e^{in\Phi_n^*} \equiv -\frac{\langle r^n e^{in\phi} \rangle}{\langle r^n \rangle}$$

Hydro-response

Space-time dynamics

Particle flow

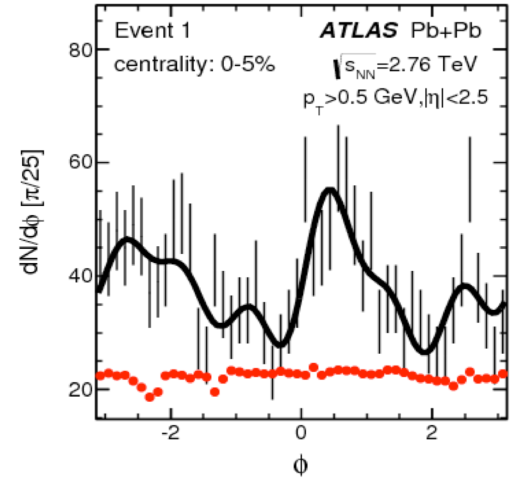

$$\frac{dN}{d\phi} \propto 1 + 2\sum_n v_n \cos n(\phi - \Phi_n)$$

Perturbing the system with different initial state fluctuations

Richness of flow fluctuations

Event by event fluctuations

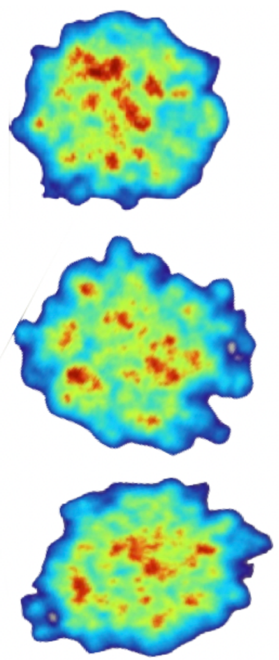

Fluctuations within a single event

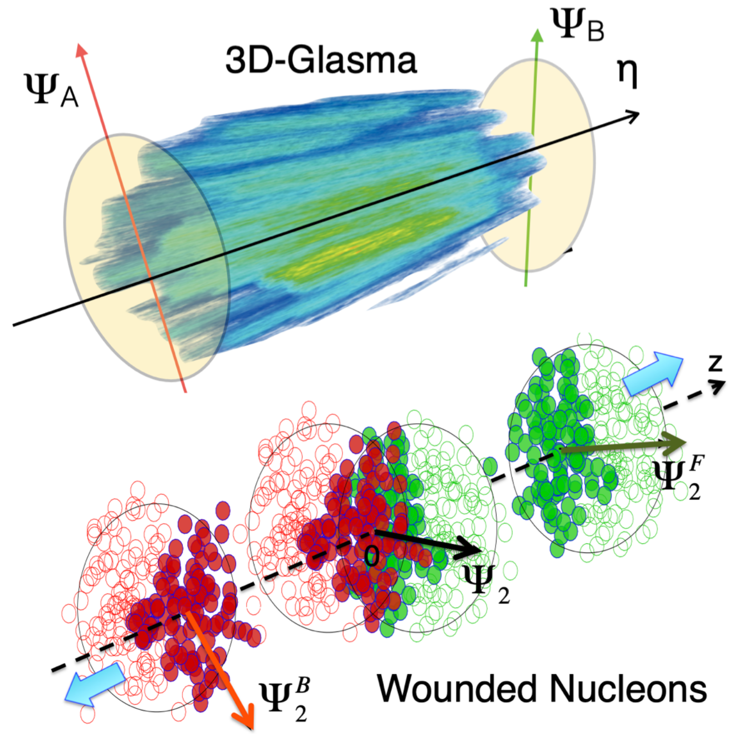

$$\frac{dN}{d\phi} \propto 1 + 2\sum_n v_n(p_T,\eta,\ldots)\cos n\left(\phi - \Phi_n(p_T,\eta,\ldots)\right) \text{ + noise}$$

$\sim 1/\sqrt{N}$

How do we analyze this object?

Flow observables arXiv: 1407.6057

- Single particle distribution

Flow vector: $V_n = v_n e^{in\Phi_n}$

$$\frac{dN}{d\phi d\eta dp_T} = N(p_T,\eta)\left[1+2\sum_n \mathrm{v}_n(p_T,\eta)\cos n\left(\phi-\Phi_n(p_T,\eta)\right)\right] + \text{noise}$$

$$= N(p_T,\eta)\left[\sum_{n=-\infty}^{\infty} V_n(p_T,\eta)e^{in\phi}\right] + \text{noise}$$

$$N(p_T,\eta) = V_0(p_T,\eta)$$

Radial flow: $V_0(p_T,\eta)$; Anisotropic flow: $V_n(p_T,\eta)e^{in\phi}$

- Two-particle correlation function

$$\left\langle \frac{dN_1}{d\phi d\eta dp_T}\frac{dN_2}{d\phi d\eta dp_T}\right\rangle \Rightarrow \left\langle V_n(p_{T1},\eta_1)V_n^*(p_{T2},\eta_2)\right\rangle \Rightarrow v_n\{2PC\} \equiv \sqrt{\mathrm{V_n V_n^*}}$$

- Multi-particle correlation function

$$\left\langle \frac{dN_1}{d\phi d\eta dp_T}\cdot\cdot\frac{dN_m}{d\phi d\eta dp_T}\right\rangle \Rightarrow \left\langle V_{n_1}V_{n_2}\ldots V_{n_m}\right\rangle \quad n_1+n_2+\ldots+n_m=0$$

$$\downarrow$$

$$\langle v_{n_1}v_{n_2}\ldots v_{n_m}\cos(n_1\Phi_{n_1}+n_2\Phi_{n_2}+\ldots+n_m\Phi_{n_m})\rangle$$

Flow observables arXiv: 1407.6057

- Single particle distribution

Flow vector: $V_n = v_n e^{in\Phi_n}$

$$\frac{dN}{d\phi d\eta dp_T} = N(p_T,\eta)\left[1+2\sum_n \mathrm{v}_n(p_T,\eta)\cos n\left(\phi-\Phi_n(p_T,\eta)\right)\right] + \text{noise}$$

$$= N(p_T,\eta)\left[\sum_{n=-\infty}^{\infty} V_n(p_T,\eta)e^{in\phi}\right] + \text{noise}$$

$N(p_T,\eta) = V_0(p_T,\eta)$

Radial flow → $V_0(p_T,\eta)$; Anisotropic flow → $V_n(p_T,\eta)$

- Two-particle correlation function

$$\left\langle \frac{dN_1}{d\phi d\eta dp_T}\frac{dN_2}{d\phi d\eta dp_T}\right\rangle \Rightarrow \left\langle V_n(p_{T1},\eta_1)V_n^*(p_{T2},\eta_2)\right\rangle \Rightarrow v_n\{2\mathrm{PC}\} \equiv \sqrt{\mathrm{V_n V_n^*}}$$

- Multi-particle correlation function

$$\left\langle \frac{dN_1}{d\phi d\eta dp_T}..\frac{dN_m}{d\phi d\eta dp_T}\right\rangle \Rightarrow \left\langle V_{n_1}V_{n_2}...V_{n_m}\right\rangle \quad n_1+n_2+...+n_m=0$$

↓

$$p(v_n, v_m, ..., \Phi_n, \Phi_m, ...) = \frac{1}{N_{\mathrm{evts}}}\frac{dN_{\mathrm{evts}}}{dv_n dv_m ... d\Phi_n d\Phi_m ...}$$

Example cumulants

- Single-flow cumulants

$$c_n\{2\} = \left\langle v_n^2 \right\rangle$$
$$c_n\{4\} = \left\langle v_n^4 \right\rangle - 2\left\langle v_n^2 \right\rangle^2$$
$$c_n\{6\} = \left\langle v_n^6 \right\rangle - 9\left\langle v_n^4 \right\rangle\left\langle v_n^2 \right\rangle + 12\left\langle v_n^2 \right\rangle^3$$
$$\cdots$$

n=1-7

- Symmetric cumulants

$$\mathrm{sc}_{n,m}\{4\} = \left\langle v_n^2 v_m^2 \right\rangle - \left\langle v_n^2 \right\rangle\left\langle v_m^2 \right\rangle$$

(n,m)=(2,3), (2,4)…

- Asymmetric cumulants (Event plane correlator)

$$\left\langle v_2^2 v_4 \cos 4(\Psi_2 - \Psi_4) \right\rangle$$
$$\left\langle v_2^3 v_3^2 \cos 6(\Psi_2 - \Psi_3) \right\rangle$$
$$\left\langle v_2 v_3 v_5 \cos(2\Psi_2 + 3\Psi_3 - 5\Psi_5) \right\rangle$$
$$\cdots$$

See Y. Zhou’s talk last week

- v_n-v_0 correlators $\left\langle v_n^2 \, N \right\rangle$, $\left\langle v_n^2 \, \delta p_{\mathrm{T}} \right\rangle$ …

$$\left\langle \delta p_{\mathrm{T}} \delta p_{\mathrm{T}} \right\rangle, \left\langle \delta p_{\mathrm{T}} \delta p_{\mathrm{T}} \delta p_{\mathrm{T}} \right\rangle \ \ldots$$

ATLAS Detector

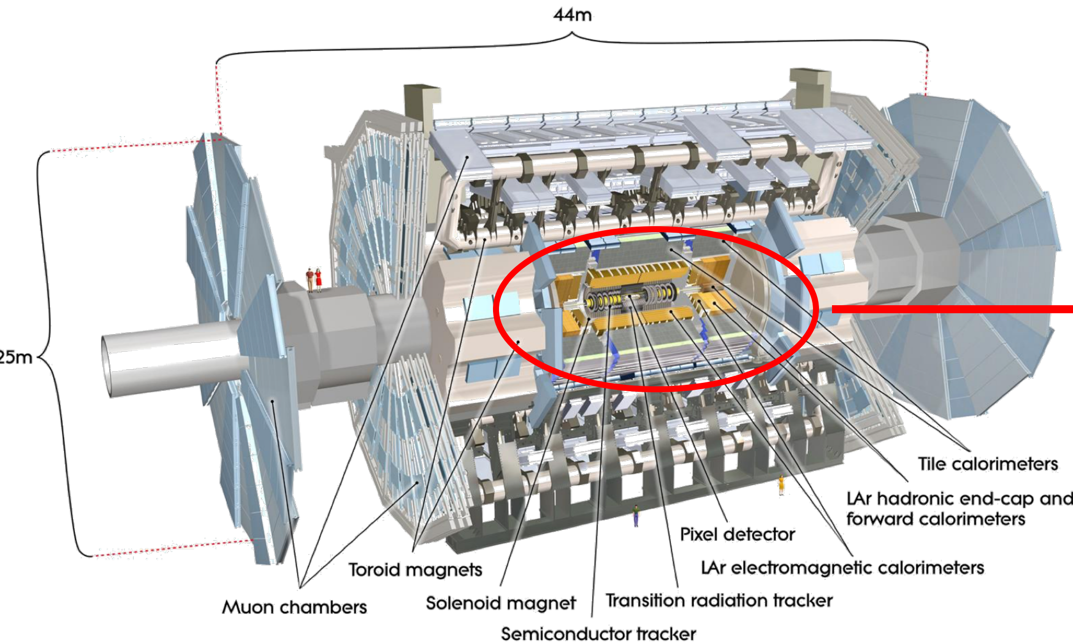

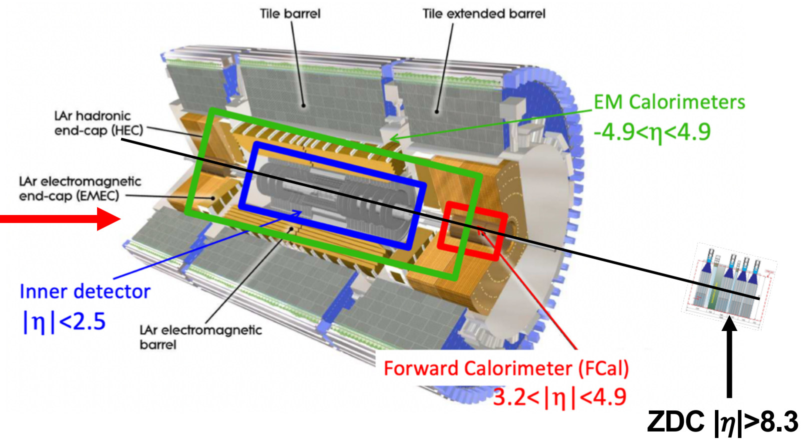

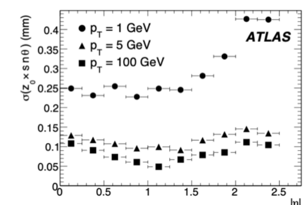

high p_T

Tracking: $r\phi \times z$ resolution ~10 × 90μm, $\sigma\left(\frac{1}{p_T}\right) = \frac{1}{340}\left(1 \oplus \frac{44\text{-}80}{p_T}\right)$

Identification for $e^{\pm}$ and V0 decays

Low p_T hadron PID via dE/dx

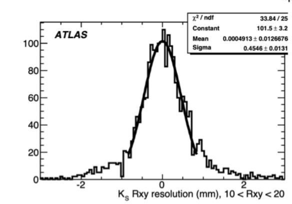

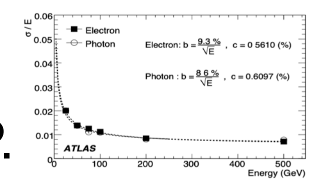

Calorimeters: high energy and position resolution

high $r\phi \times z$ granularity important for EP.

ZDC with RP capability

Jet flow and higher v_n

Longitudinal correlation

Muon spectrometer: large acceptance for $\mu^{\pm}$

Heavy flavor and quarkonium flow

ATLAS Triggers

Selection of interesting events up to 1/30,000 with high efficiency

→ Achieved by combination of L1 and HLT trigger, critical especially in pp and pPb

Pileup rejection

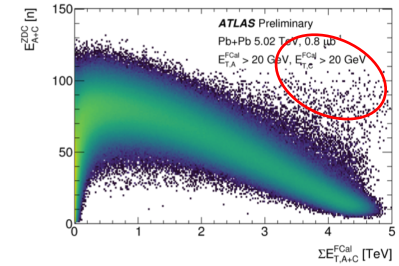

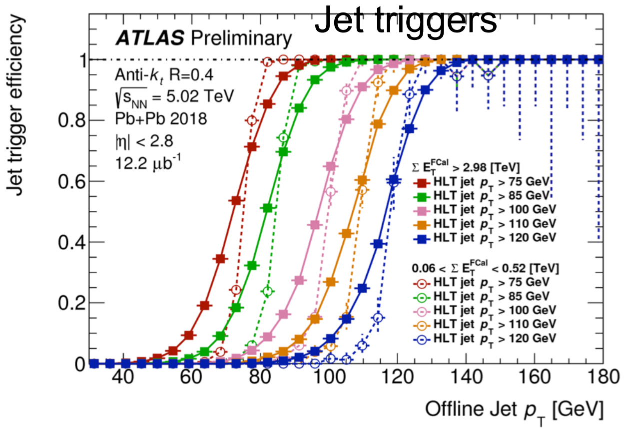

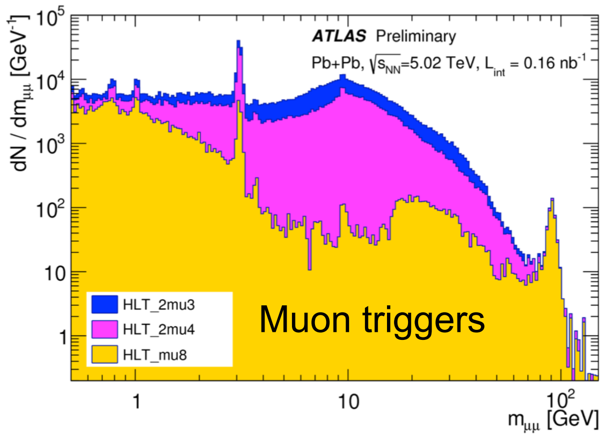

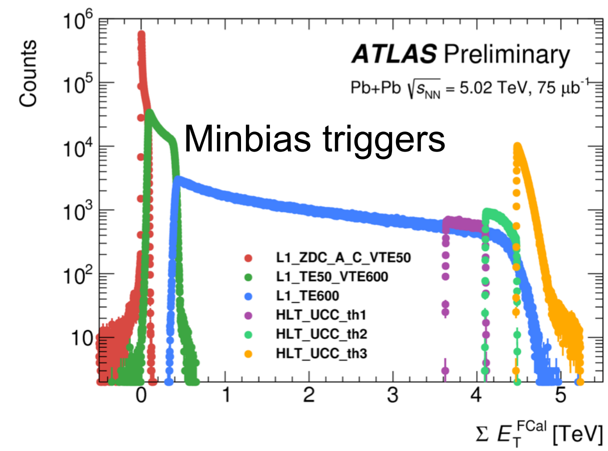

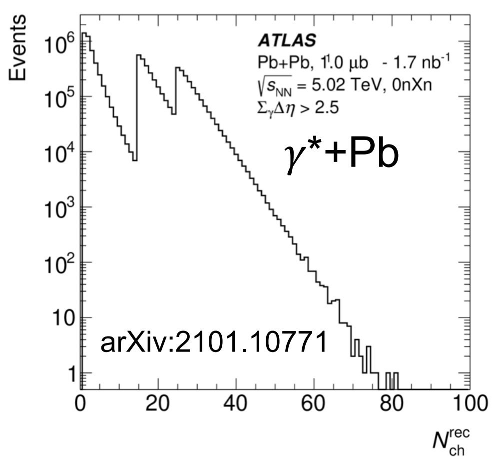

High multiplicity triggers

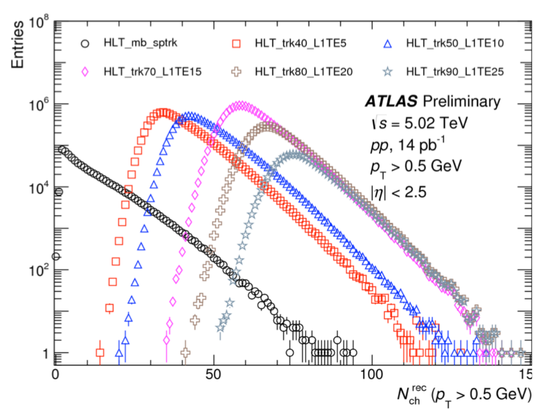

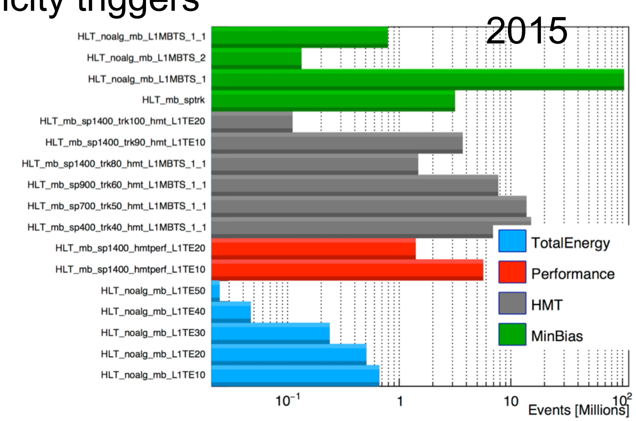

ATLAS capability for flow measurements

$$v_n = \frac{\langle \cos(n(\phi - \Psi_n))\rangle}{\mathrm{Res}\{\Psi_\mathrm{n}\}}$$

$$\mathrm{Res}\{\Psi_\mathrm{n}\} = \langle \cos(n(\Psi_n - \Psi_{n,\mathrm{true}}))\rangle$$

$$p(V_n) \propto \exp\left(-\frac{(v_{\mathrm{nx}} - v_{\mathrm{nrp}})^2 + v_{\mathrm{ny}}^2}{\sigma^2}\right)$$

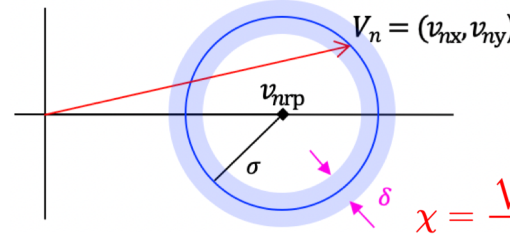

$$\chi = \frac{\sqrt{v_{n,\mathrm{rp}}^2 + \sigma^2}}{\delta}$$

Large and flexible set of choices of detectors for correlations

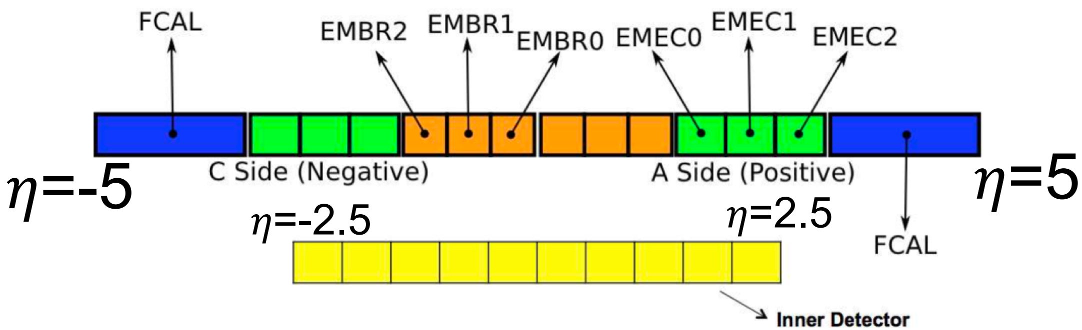

Detector	Name	Description	$\vert\eta\vert$ coverage	Calorimeter-Layers
1	EMB0	EMcal Barrel	0-0.5	presamp+layer1,2
2	EMB1	EMcal Barrel	0.5-1.5	presamp+layer1,2
3	EMB2	EM Barrel	0-1.5	sum of Detectors 1 and 2
4	EME0	EMcal End Cap	1.5-2.1	presamp+layer1,2
5	EME1	EMcal End Cap	1.5-2.7	Detector 4 +
				presamp+layer1,2,3 for $2.1 < \eta < 2.7$
6	EME2	EMcal End Cap	1.5-3.2	Detector 4+
				presamp+layer1,2 for $2.7 < \eta < 3.2$
7	EMB1EME0	EM Barrel + End Cap	0.5-2.1	sum of Detectors 2 and 4
8	ID0	Inner Detector	0.5-2.0	charged particles $p_T > 0.5$ GeV
9	ID1	Inner Detector	0-2.5	charged particles $p_T > 0.5$ GeV

Table 2: Detectors used in the three sub-event method to determine Full-FCal and Sub-Fcal resolution. If only one side of the detector is used, we use a substript "N" or "P" to indicate the either negative or the positive η.

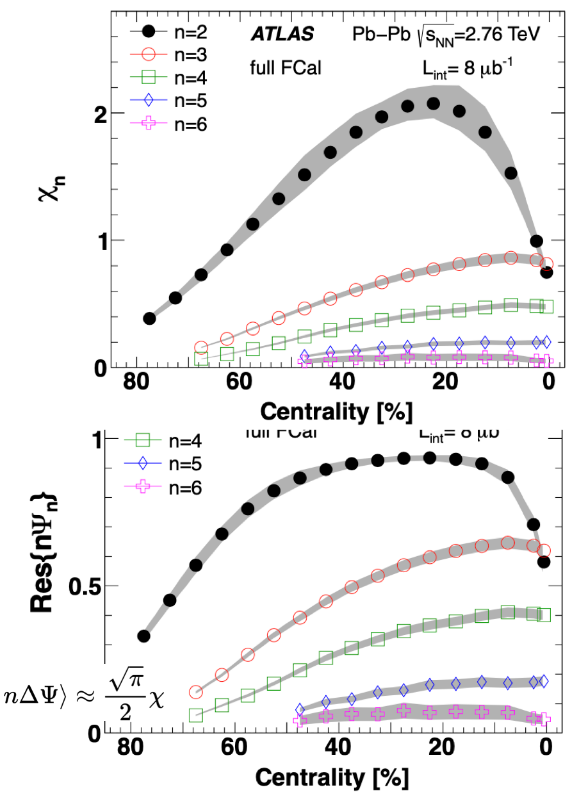

$$\langle \cos n\Delta\Psi\rangle \approx \frac{\sqrt{\pi}}{2}\chi$$

Detector nonuniformity

FCal Energy distribution in lab frame

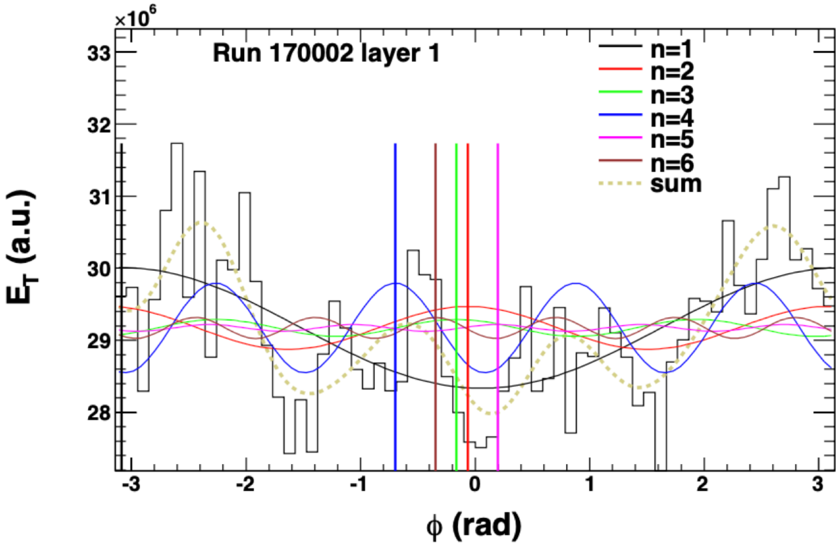

$$\langle \frac{dE_T}{d\phi} \rangle = Q_0 + 2\sum_{n=1}^{\infty}(\langle Q_{x,n}^{raw}\rangle \cos(n\phi) + \langle Q_{y,n}^{raw}\rangle \sin(n\phi))$$

Phases independent of centrality

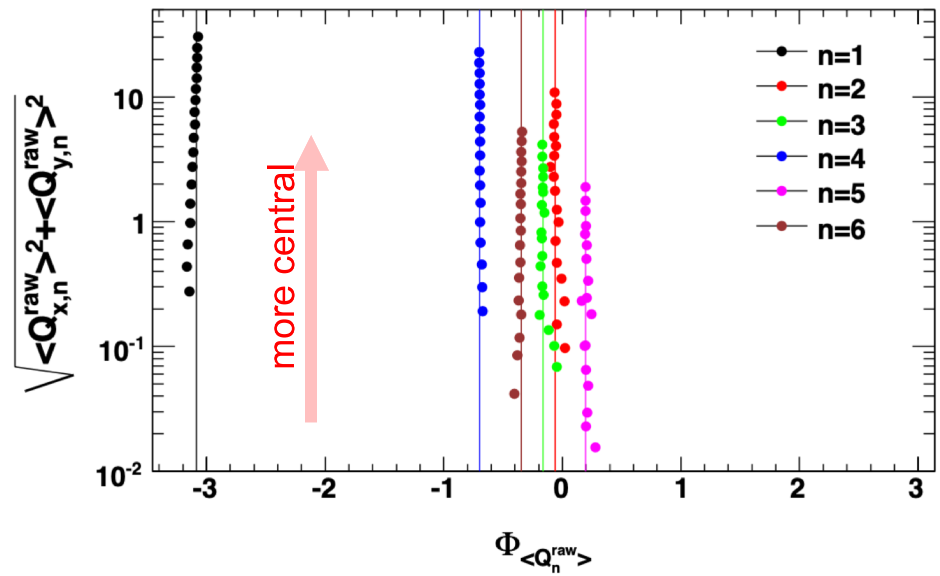

$$\overline{Q_n^{raw}} = \sqrt{\langle Q_{x,n}^{raw}\rangle^2 + \langle Q_{y,n}^{raw}\rangle^2}, \quad \Phi_n = \frac{1}{n}\tan^{-1}\left(\frac{\langle Q_{y,n}^{raw}\rangle}{\langle Q_{x,n}^{raw}\rangle}\right)$$

Simple offset and shift correction

$$Q_{x,n} = \frac{Q_{x,n}^{raw} - \langle Q_{x,n}^{raw}\rangle}{\sigma_{Q_{x,n}^{raw}}}, \quad Q_{y,n} = \frac{Q_{y,n}^{raw} - \langle Q_{y,n}^{raw}\rangle}{\sigma_{Q_{y,n}^{raw}}}$$

$$\Psi_n \rightarrow \Psi_n + \delta\Psi_n,$$

$$n\delta\Psi_n = \sum_{k=1}^{k_{max}} \frac{2}{k}\left[-\langle \sin(kn\Psi_n)\rangle \cos(kn\Psi_n) + \langle \cos(kn\Psi_n)\rangle \sin(kn\Psi_n)\right]$$

A.M. Poskanzer and S. A. Voloshin
Phys. Rev. C 58, 1671

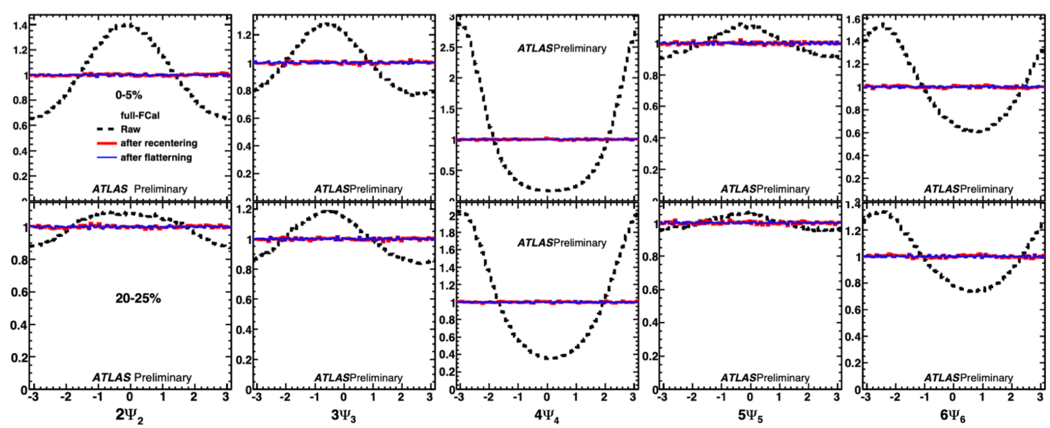

$v_n(\text{cent}, p_T, \eta)$ via the Event plane method

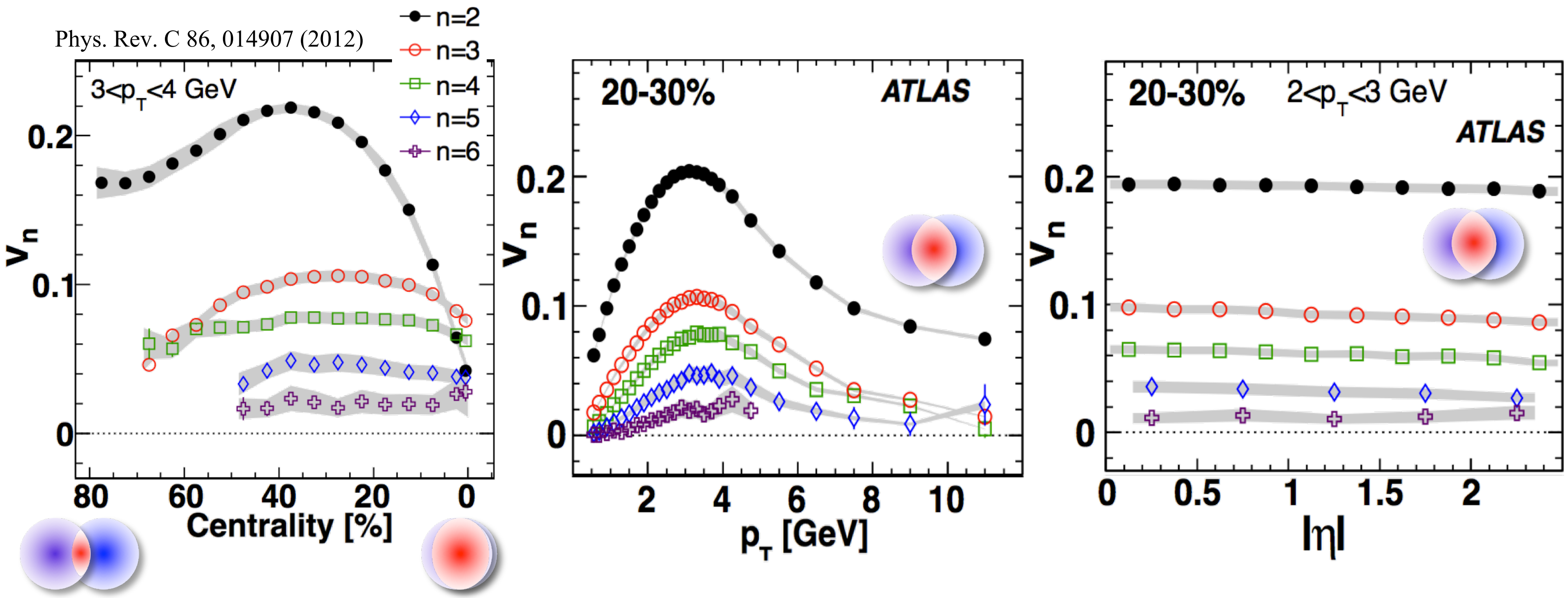

- Features of Fourier coefficients
  - v_n coefficients rise and fall with centrality.
  - v_n coefficients rise and fall with p_T.
  - v_n coefficients are ~boost invariant.

Flow correlations are geometric and long range!

Two-particle correlation method

Signal distribution

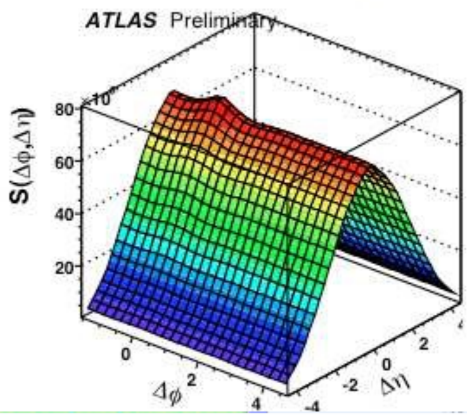

background distribution

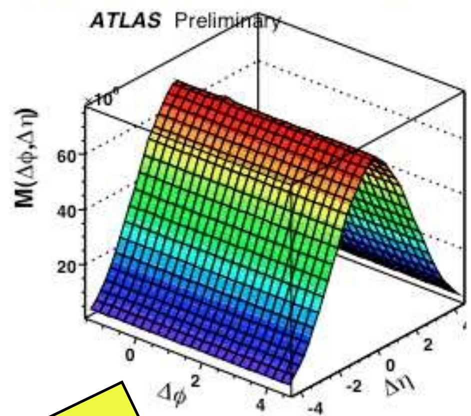

Correlation function S/B

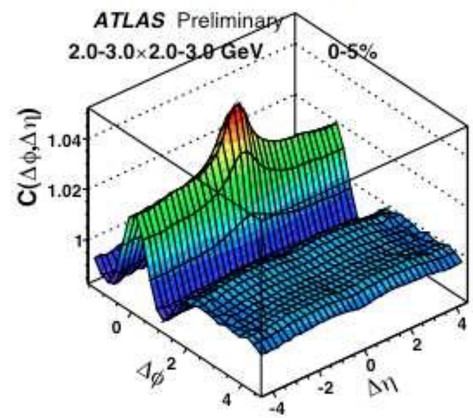

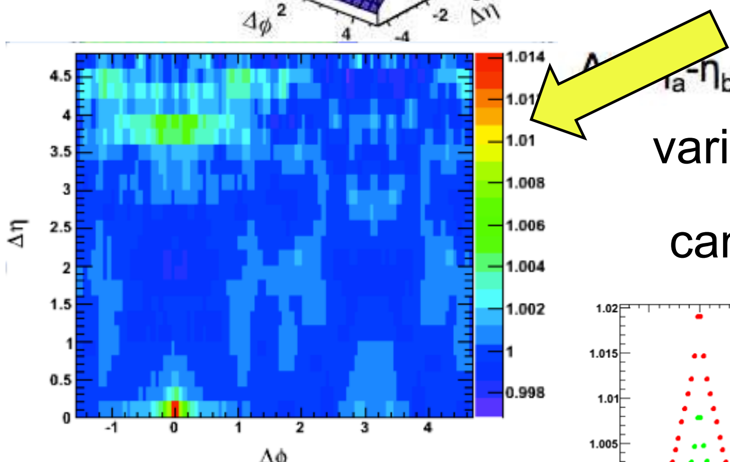

Renormalize in each $\Delta\eta$ slice

variation in $\Delta\phi$ is < 0.5% except at around $\Delta\eta$, $\Delta\phi$~0.

cancelled out by mixed-event pairs

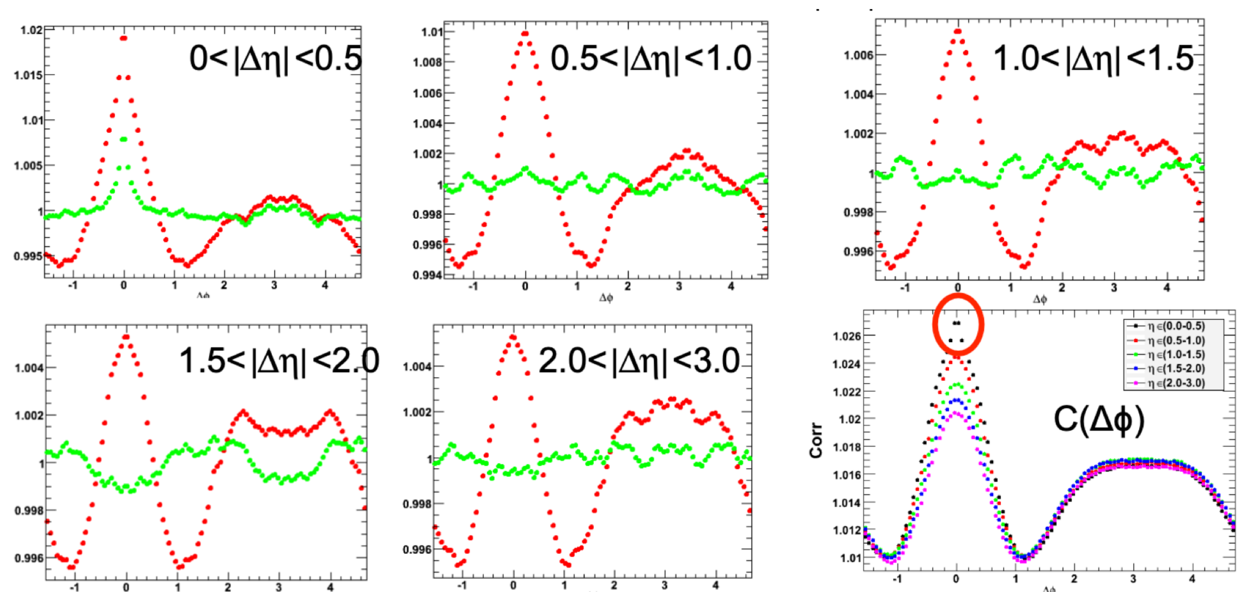

Effects of residual detector effects

- For each event, make the foreground ab pairs. Mixed event: a with b from a random event with similar centrality (5%) and z-vertex (0.5cm).
- Three checks were done for the pair acceptance
  - Time dependence→vary the event gap and check the result
  - Centrality matching→vary the width of the centrality bin for mixing
  - Z-vertex matching→vary the width of zbin for mixing.

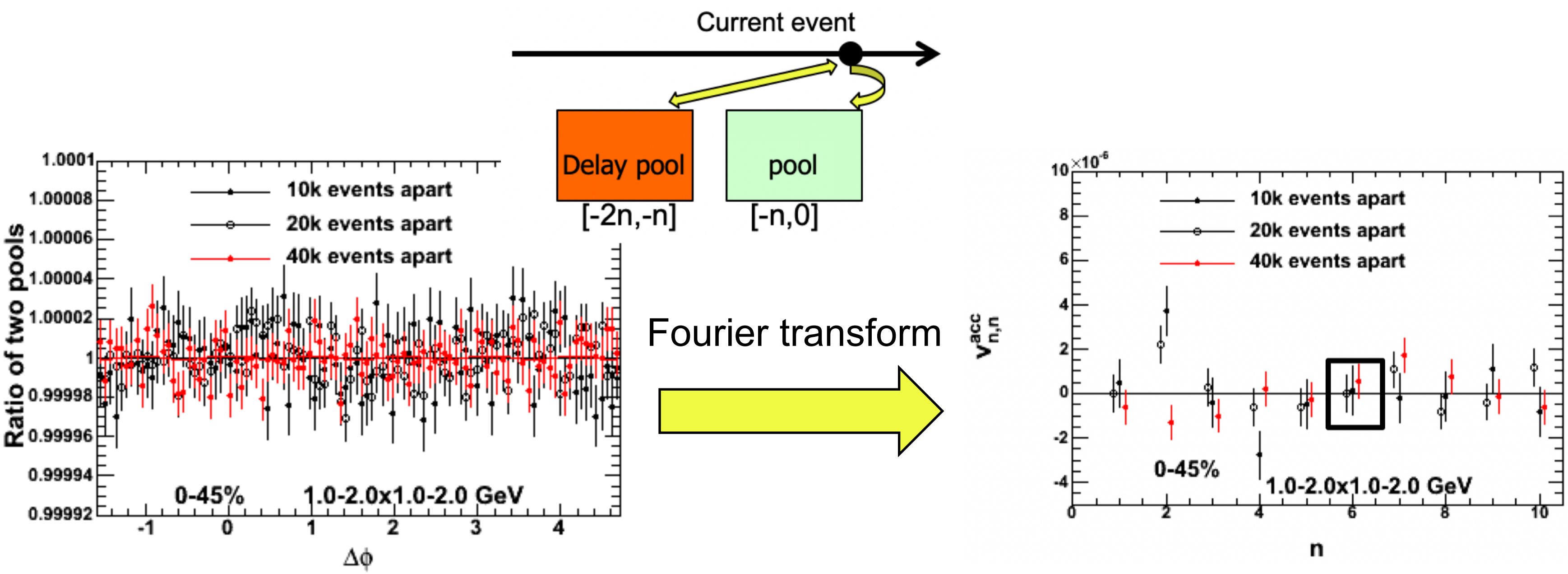

Effects of residual detector effects

- For each event, make the foreground ab pairs. Mixed event: a with b from a random event with similar centrality (5%) and z-vertex (0.5cm).
- Three checks were done for the pair acceptance
  - Time dependence→vary the event gap and check the result
  - Centrality matching→vary the width of the centrality bin for mixing
  - Z-vertex matching→vary the width of zbin for mixing.

results with different z vertex binning: 25, 20,15,10,5,2.5 and 1mm match with the mixed event. See some convergence (already pretty good with 5mm), the error band is around 2×10^{-6}.

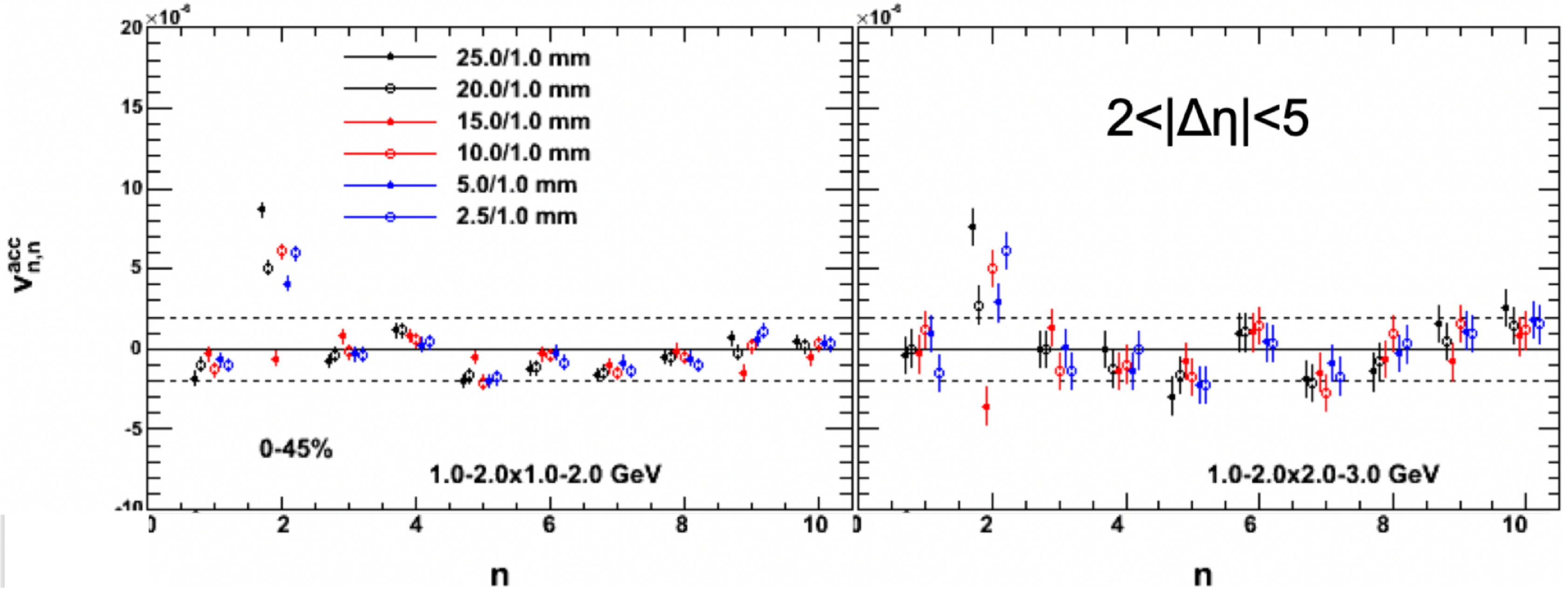

v_n via two-particle correlations

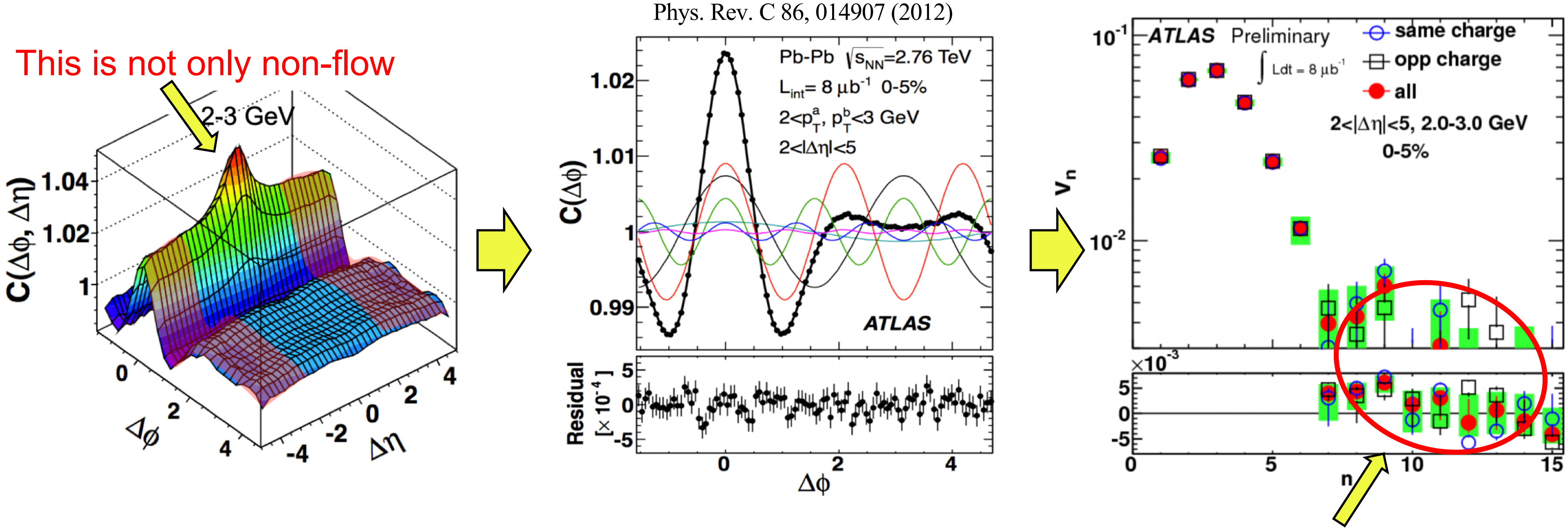

Are there higher-order harmonics?

- Long range structures (“ridge”) described by harmonics $v_{1,1}$-$v_{6,6}$

$$\frac{dN}{d\Delta\phi} \propto 1 + \sum_n 2 v_{n,n}\left(p_T^a, p_T^b\right)\cos\left(n\Delta\phi\right) \qquad v_{n,n}(\mathbf{p}_T^a, \mathbf{p}_T^b) = \mathbf{v}_n(\mathbf{p}_T^a)\mathbf{v}_n(\mathbf{p}_T^b)$$

Flow fluctuations and their power

arXiv:1305.2942

Gale, Jeon, Schenke, Tribedy, Venugopalan 1209.6330

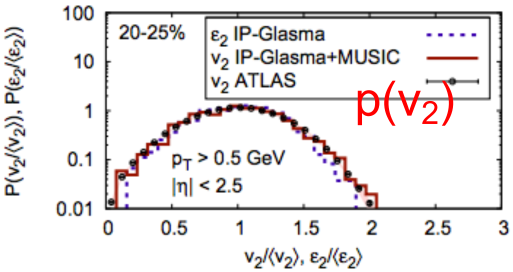

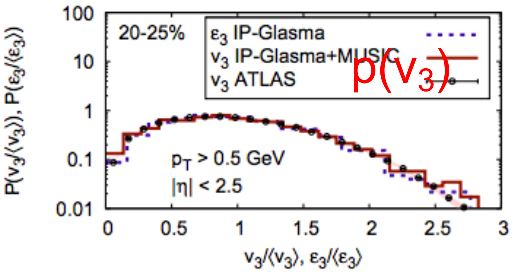

arXiv: 1403.0489,

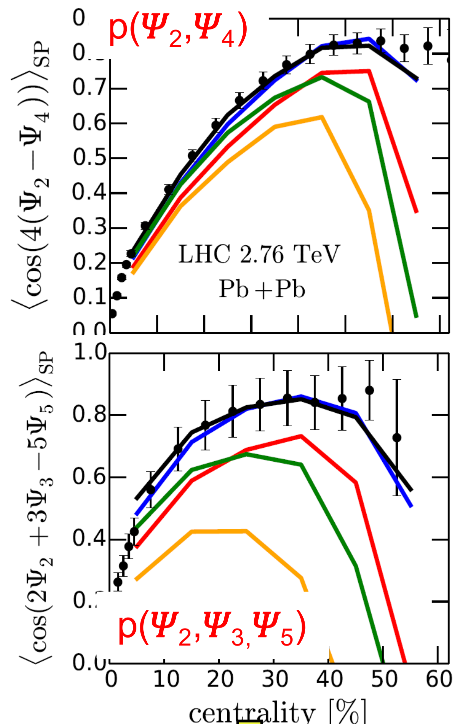

arXiv: 1504.01289

$p(v_2,v_3)$, $p(v_2,v_4)$

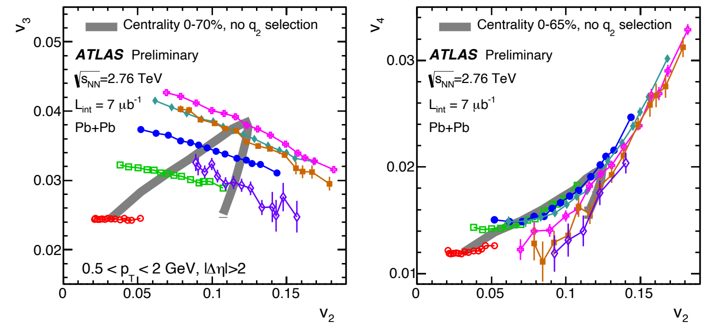

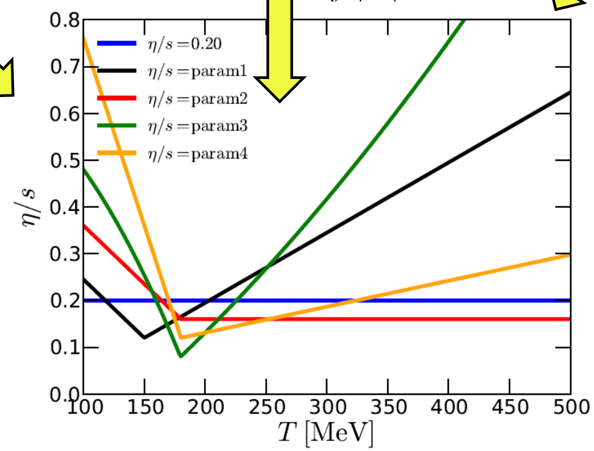

Niemi, Eskola, Paatelainen 1505.02677

Probe the hydrodynamic response: $(\varepsilon_n, \Phi_n) \rightarrow (v_n, \Psi_n)$

Sensitive to detail of transport coeffis: $\eta/s(T)$

Disentangle the initial and final state effects

How to measure event plane correlation?

- We use scalar product method, which approximately gives

$$\langle\cos(c_1\Phi_1 + ... + lc_l\Phi_l)\rangle = \frac{\langle\cos(c_1\Psi_1 + ... + lc_l\Psi_l)\rangle}{\text{Res}\{c_1\Psi_1\}...\text{Res}\{c_l l\Psi_l\}}$$

$$\text{Res}\{c_n n\Psi_n\} = \langle\cos c_n n(\Psi_n - \Phi_n)\rangle$$

$$c_1 + 2c_2 ... + lc_l = 0$$

$$\approx \frac{\left\langle v_1^{c_1} v_2^{c_2} \ldots v_l^{c_l} \cos(c_1\Psi_1 + 2c_2\Psi_2 + \ldots + lc_l\Phi_l)\right\rangle}{\sqrt{\left\langle v_1^{2c_1}\right\rangle \left\langle v_2^{2c_2}\right\rangle \ldots \left\langle v_l^{2c_l}\right\rangle}}$$

Taken from different subevents

- Sensitivity limit is set by the resolution Res{}

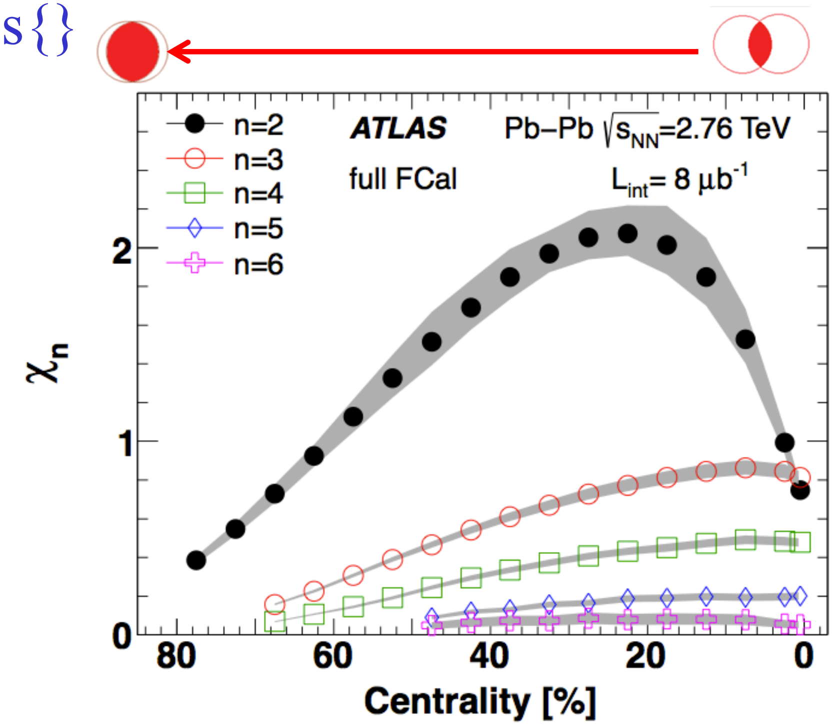

Jean-Yves Ollitrault
Phys. Rev. D 46, 229

$$\text{Res}\{jn\Psi_n\} = \langle\cos jn(\Psi_n - \Phi_n)\rangle$$

$$= \frac{\chi_n\sqrt{\pi}}{2} e^{-\frac{\chi_n^2}{2}} \left[I_{(j-1)/2}(\frac{\chi_n^2}{2}) + I_{(j+1)/2}(\frac{\chi_n^2}{2}) \right]$$

$$\approx \begin{cases} 1 - \frac{j^2}{8z} + \frac{j^2(j^2-4)}{128z^2}, z = \chi_n^2/2 & \text{for large } \chi_n \\ \frac{\sqrt{\pi}}{2^j\Gamma(\frac{j+1}{2})}\chi_n^j & \text{for small } \chi_n \end{cases}$$

- χ_n, thus Res{}, decreases fast with n
- Decrease slower with j, especially if χ_n is large

EP correlation for alignment

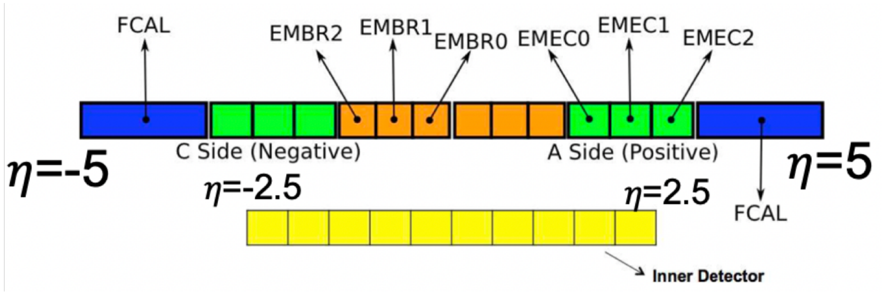

A rotation between two subevents will show up in correlations

$$\frac{\langle \sin k(\Psi_n^{\mathrm{N}} - \Psi_n^{\mathrm{P}} + \delta) \rangle}{\langle \cos k(\Psi_n^{\mathrm{N}} - \Psi_n^{\mathrm{P}} + \delta) \rangle} \approx \tan k\delta \approx k\delta$$

Detector response phase-shift between + and - side, revealed by flow

$$\frac{dN}{d\Delta\Psi} \propto 1 + 2v_n f(\Delta\Psi + \delta)$$

see the rotation δ only if signal is non-zero.

Can not correct via mixed-event, since v_n=0 in mixed-event.

Forward $\delta \approx 0.01$

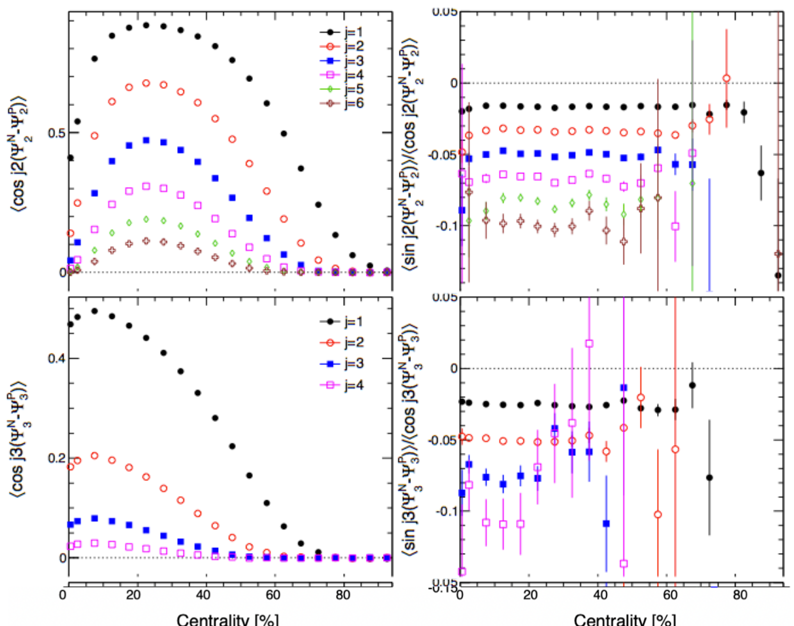

Center $\delta \approx 0$

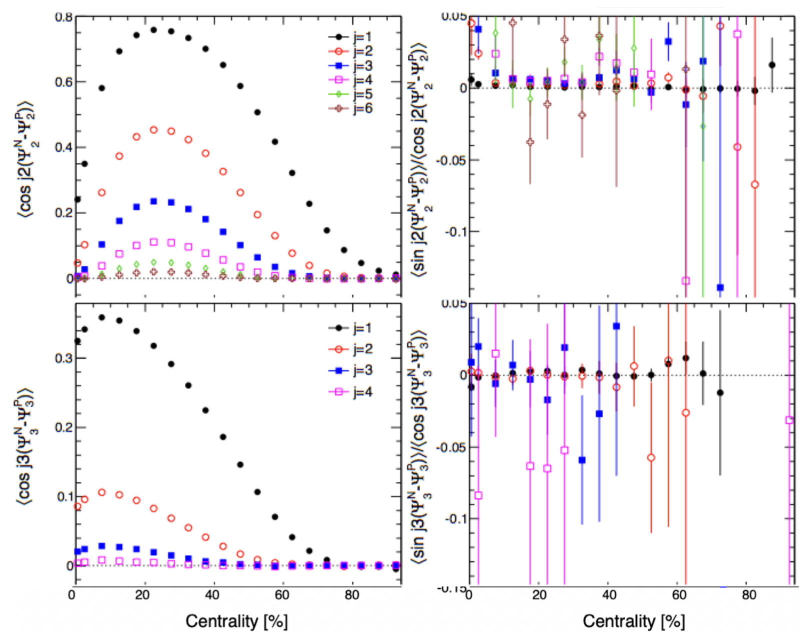

For illustration purpose

Results and interpretation

$$\frac{\langle v_1^{c_1} v_2^{c_2} \ldots v_l^{c_l} \cos(c_1\Psi_1 + 2c_2\Psi_2 + \ldots + lc_l\Phi_l)\rangle}{\sqrt{\langle v_1^{2c_1}\rangle\langle v_2^{2c_2}\rangle \ldots \langle v_l^{2c_l}\rangle}}$$

$$V_n = v_n e^{in\Psi_n}$$

$$\frac{\langle \epsilon_1^{c_1}\epsilon_2^{c_2} \ldots \epsilon_l^{c_l} \cos(c_1\Phi_1^* + 2c_2\Phi_2^* + \ldots + lc_l\Phi_l^*)\rangle}{\sqrt{\langle \epsilon_1^{2c_1}\rangle\langle \epsilon_2^{2c_2}\rangle \ldots \langle \epsilon_l^{2c_l}\rangle}}$$

$$\mathcal{E}_n = \varepsilon_n e^{in\Phi_n}$$

$$V_{nL} \propto \mathcal{E}_n$$

$\langle\cos(2\Psi_2 + 3\Psi_3 - 5\Psi_5)\rangle$ $\langle\cos(2\Psi_2 + 4\Psi_4 - 6\Psi_6)\rangle$ $\langle\cos(2\Psi_2 - 6\Psi_3 + 4\Psi_4)\rangle$

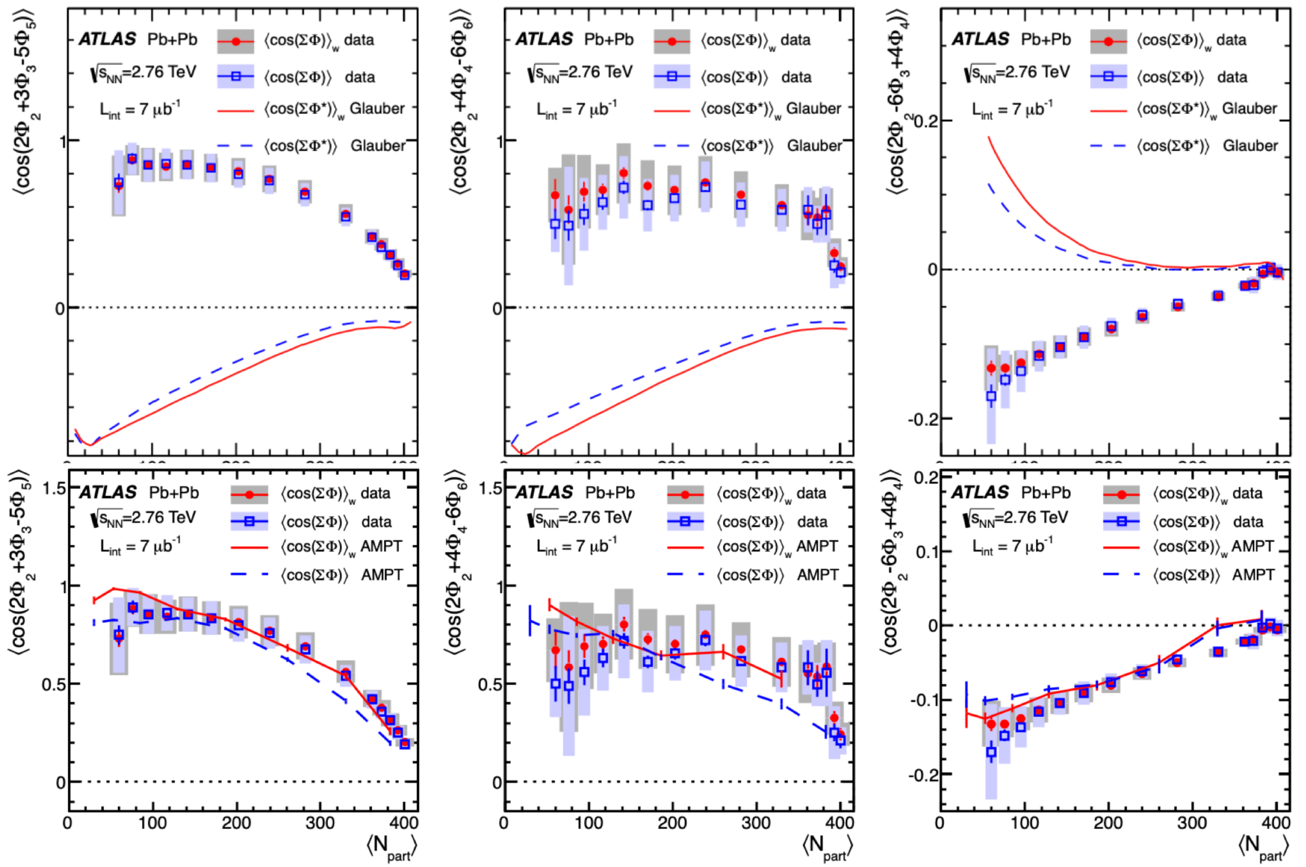

Glauber model fails ,while hydrodynamics (AMPT) model works

Indicating importance of non-linear responses:

Teany & Yan arXiv:1312.3689

$$V_4 = V_{4L} + \chi_4 (V_2)^2$$
$$V_5 = V_{5L} + \chi_5 V_2 V_3$$

$$v_4 e^{i4\Psi_4} \approx c_0 \epsilon_4 e^{i4\Phi_4} + \chi_4 v_2^2 e^{i4\Psi_2}$$
$$v_5 e^{i5\Psi_5} \approx c_1 \epsilon_5 e^{i5\Phi_5} + \chi_5 v_2 v_3 e^{i(2\Psi_2 + 3\Psi_3)}$$

Two plane correlations

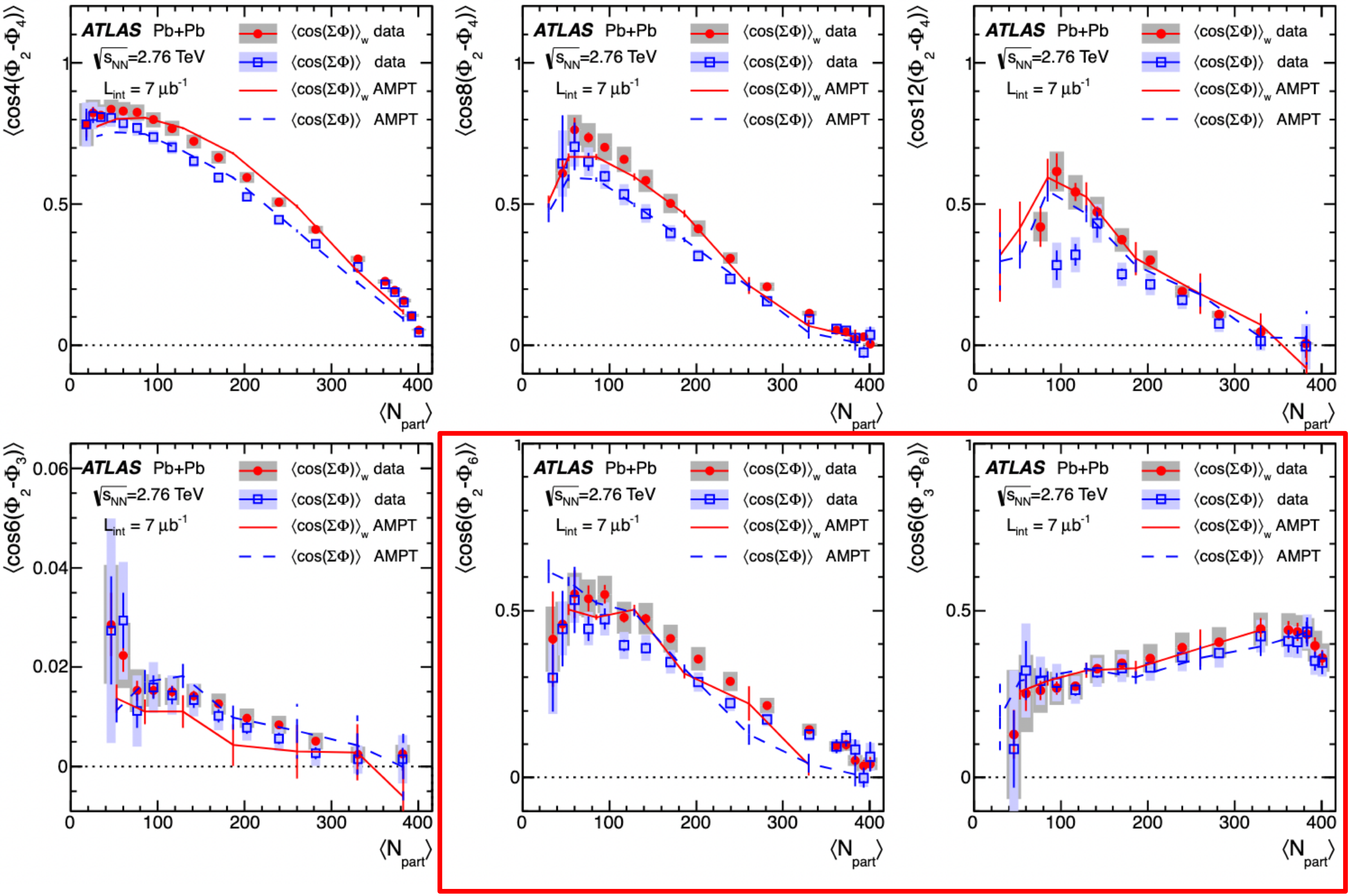

$$V_6 = V_{6\,\mathrm{L}} + \chi_{62} V_2^3 + \chi_{63} V_3^2 \quad \Rightarrow \quad v_6 e^{i6\Psi_6} \approx c_1 e^{i6\Phi_6} + \chi_{62} v_2^3 e^{i6\Psi_2} + \chi_{63} v_3^2 e^{i6\Psi_3}$$

Extraction of $p(v_n)$

arXiv:1305.2942

Flow shows up in each events

Single particle distribution:

Two-particle distribution:

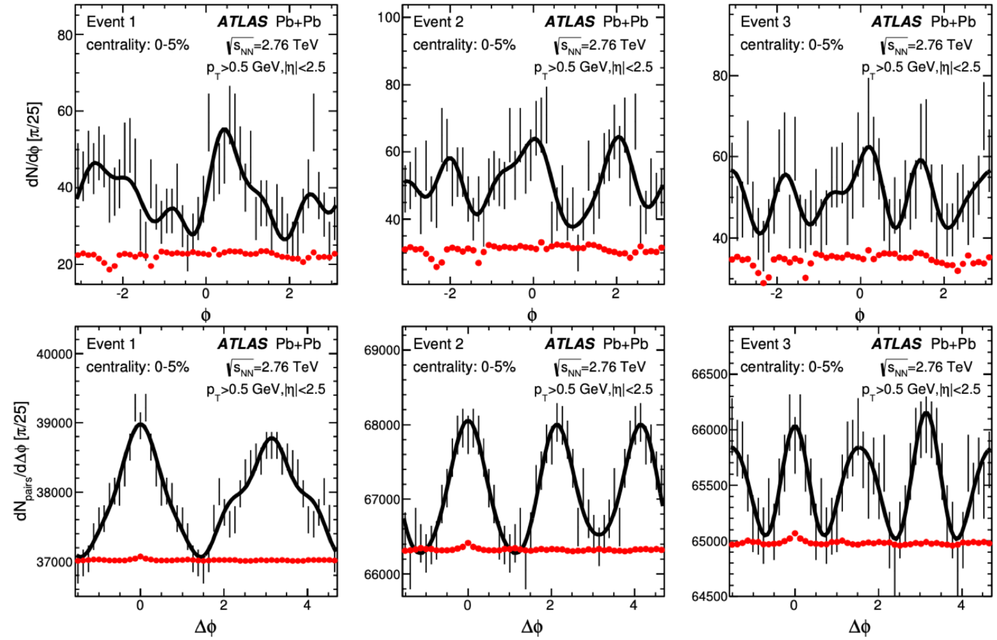

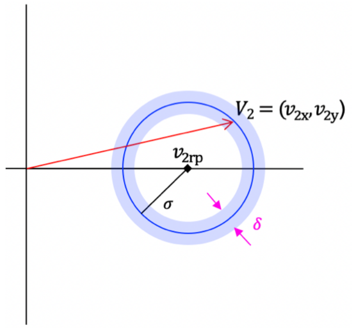

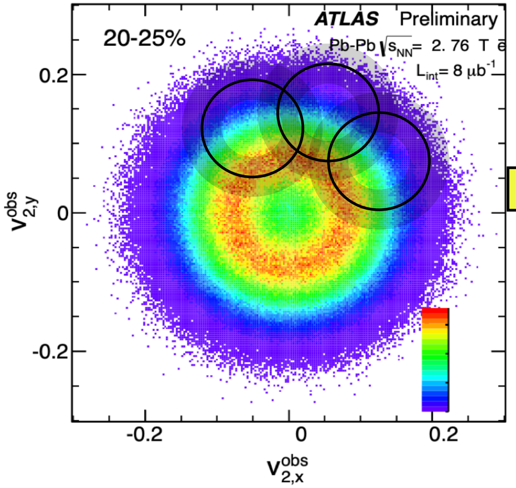

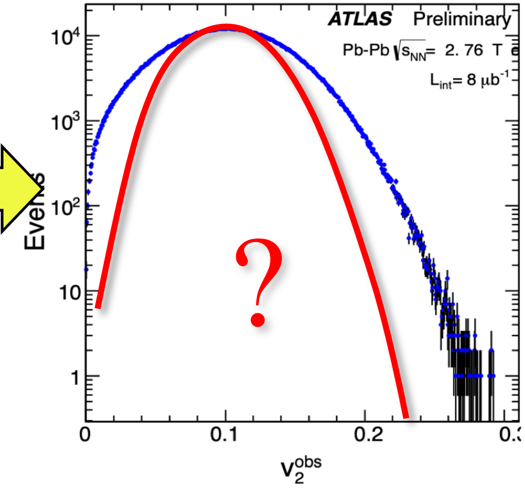

Obtaining $p(v_n)$ via unfolding

- Flow vector in each event has flow and smearing contribution

$$\boldsymbol{q}_n = \boldsymbol{v}_n + \boldsymbol{s}_\mathrm{n} \qquad p(\boldsymbol{q}_n) = p(\boldsymbol{v}_n) \otimes p(\boldsymbol{s}_n)$$

- Estimating statistical smearing from sub-events

1304.1417,1305.2942

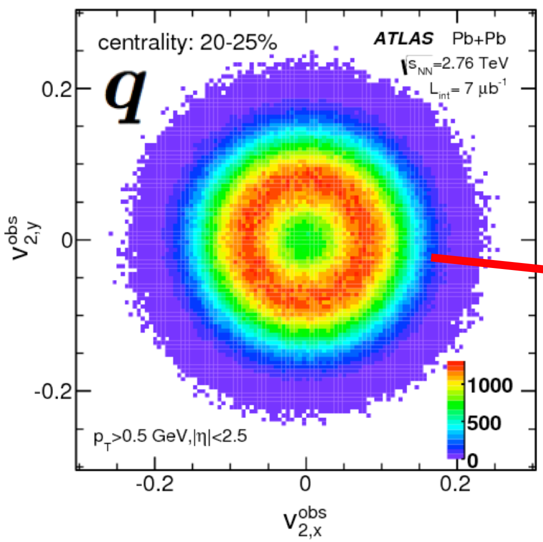

$$\boldsymbol{v} = \boldsymbol{q} - \boldsymbol{s}$$

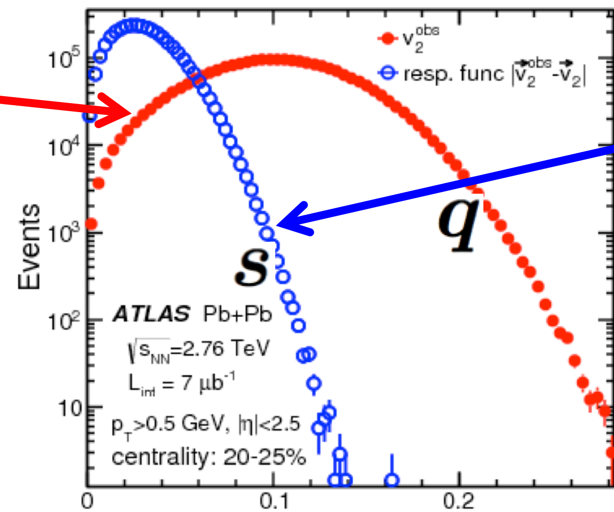

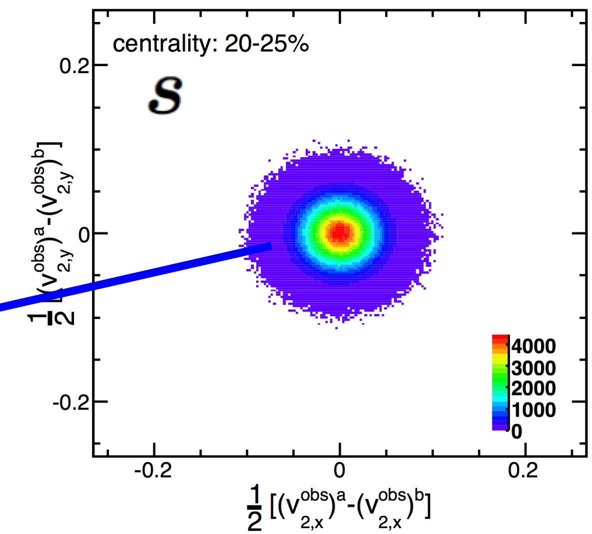

$$\boldsymbol{q} = \left[\boldsymbol{q}^\mathrm{A} + \boldsymbol{q}^\mathrm{B}\right]/2 \qquad \boldsymbol{s} \simeq \left[\boldsymbol{q}^\mathrm{A} - \boldsymbol{q}^\mathrm{B}\right]/2$$

$$= \text{nonflow} + \boldsymbol{v} \qquad = \text{nonflow}$$

"Unsmear" $p(q_n)$ by $p(s_n)$ to get $p(v_n)$

Bayesian unfolding

- unfolding algorithm as implemented in the RooUnfold
  - True ("cause" c or v_n) vs measured distribution ("effect" e or v_n^{obs})

    Denote response function $A_{ji} = p(e_j|c_i)$

G. D'Agostini, A multidimensional unfolding method based on Bayes' theorem, Nucl. Instrum. Meth. A 362 (1995) 487 [SPIRE].

  - Unfolding matrix M is determined via iterative procedure

$$\hat{c}^{\text{iter}+1} = \hat{M}^{\text{iter}} e, \quad \hat{M}_{ij}^{\text{iter}} = \frac{A_{ji}\hat{c}_i^{\text{iter}}}{\sum_{m,k} A_{mi} A_{jk} \hat{c}_k^{\text{iter}}}$$

  - Prior, c^0, can be chosen as input v_n^{obs} distribution or it can be chosen to be closer to the truth by a simple rescaling according to the EP v_n

$$\langle v_n \rangle \leq v_n^{\text{EP}} \leq \sqrt{\langle v_n^2 \rangle} = \sqrt{\langle v_n \rangle^2 + \sigma_{v_n}^2}$$

  - Number of iterations N_{iter} adjusted according to sample statistics and binning.

Unfolding performance: v_2, 20-25%

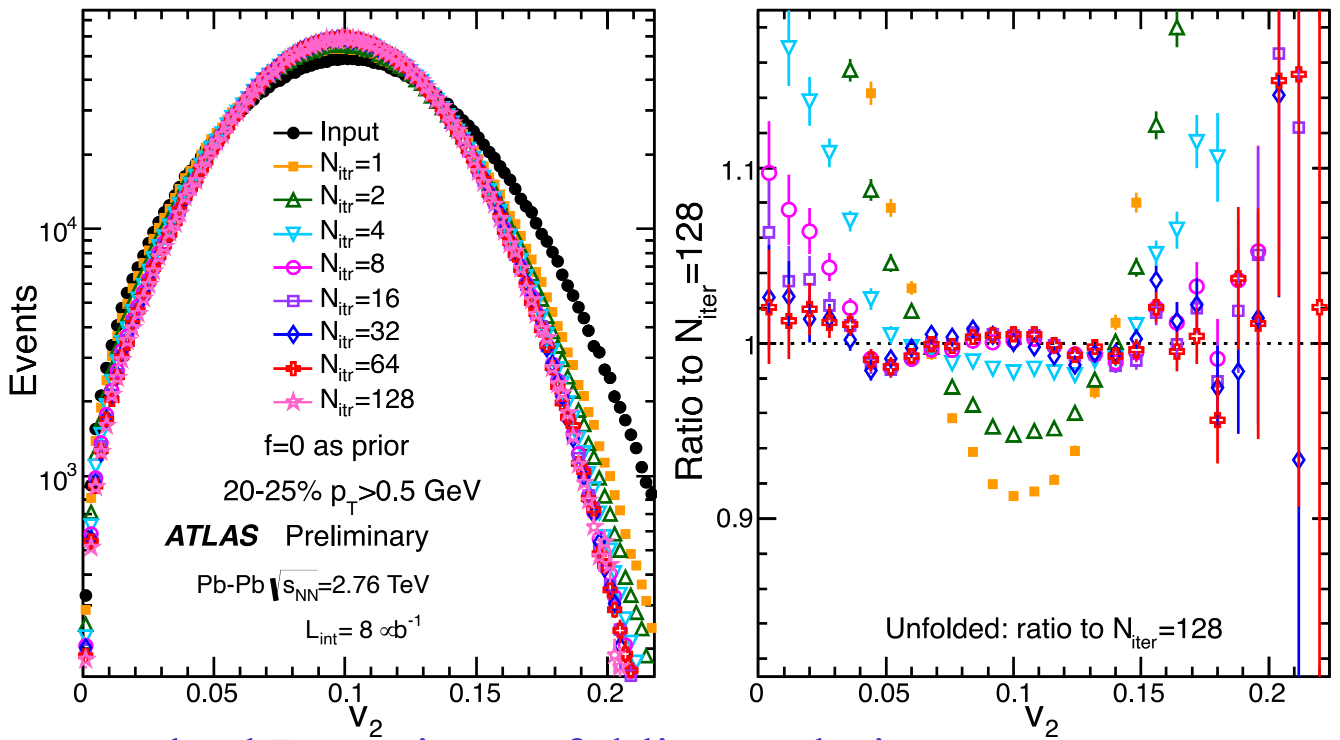

- Use the standard Bayesian unfolding technique
- Converges within a few % for N_{iter}=8, small improvements for larger N_{iter}.
- Many cross checks show good consistency
  - Unfolding with different prior distributions
  - Unfolding using tracks in a smaller detector
  - Unfolding directly on the EbE two-particle correlation.

Details in arXiv:1305.2942

Flow probability distributions

arXiv:1305.2942

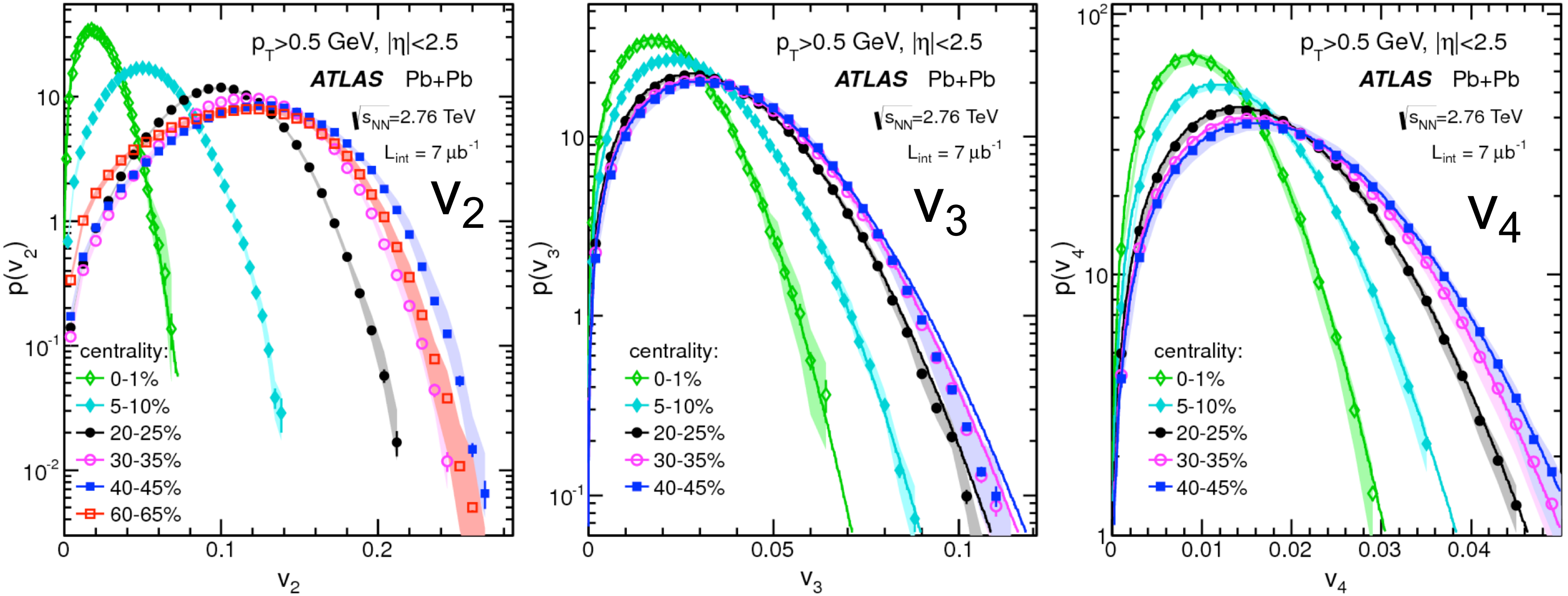

- v_2 distributions has significant reaction plane component:

$$p(v_2) = \frac{v_2}{\sigma^2} e^{-\frac{(v_2)^2 + \left(v_2^{\mathrm{RP}}\right)^2}{2\sigma^2}} I_0\left(\frac{v_2^{\mathrm{RP}} v_2}{\sigma^2}\right)$$

- v_2 in central, and v_3 v_4 in all centrality are described by a radial

Gaussian function: $P(v_n) = \frac{v_n}{\sigma^2} e^{-\frac{v_n^2}{2\sigma^2}}$ $\quad \frac{\sigma_{v_n}}{\langle v_n \rangle} = \sqrt{\frac{4}{\pi} - 1} = 0.523$

Cumulants from correlation method and from $p(v_2)$

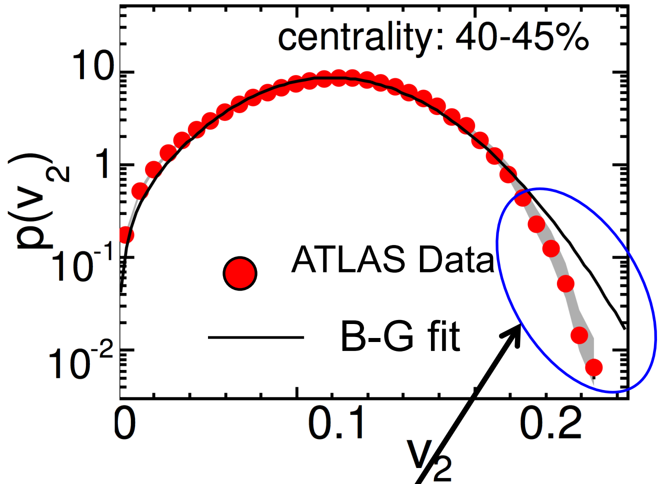

$$c_2\{4\} = \langle v_2^4 \rangle - 2\langle v_2^2 \rangle^2$$

$$c_2\{6\} = \langle v_2^6 \rangle - 9\langle v_2^4 \rangle\langle v_2^2 \rangle + 12\langle v_2^2 \rangle^3$$

$$c_2\{6\} = \langle v_2^8 \rangle - 16\langle v_2^6 \rangle\langle v_2^2 \rangle - 18\langle v_2^4 \rangle^2 + 144\langle v_2^4 \rangle\langle v_2^2 \rangle^2 - 144\langle v_2^2 \rangle^4$$

$$v_2\{4\} = \sqrt[4]{-c_2\{4\}}, v_2\{6\} = \sqrt[6]{c_2\{6\}/4}, v_2\{8\} = \sqrt[8]{-c_2\{8\}/33}$$

Non-Bessel Gaussian behavior

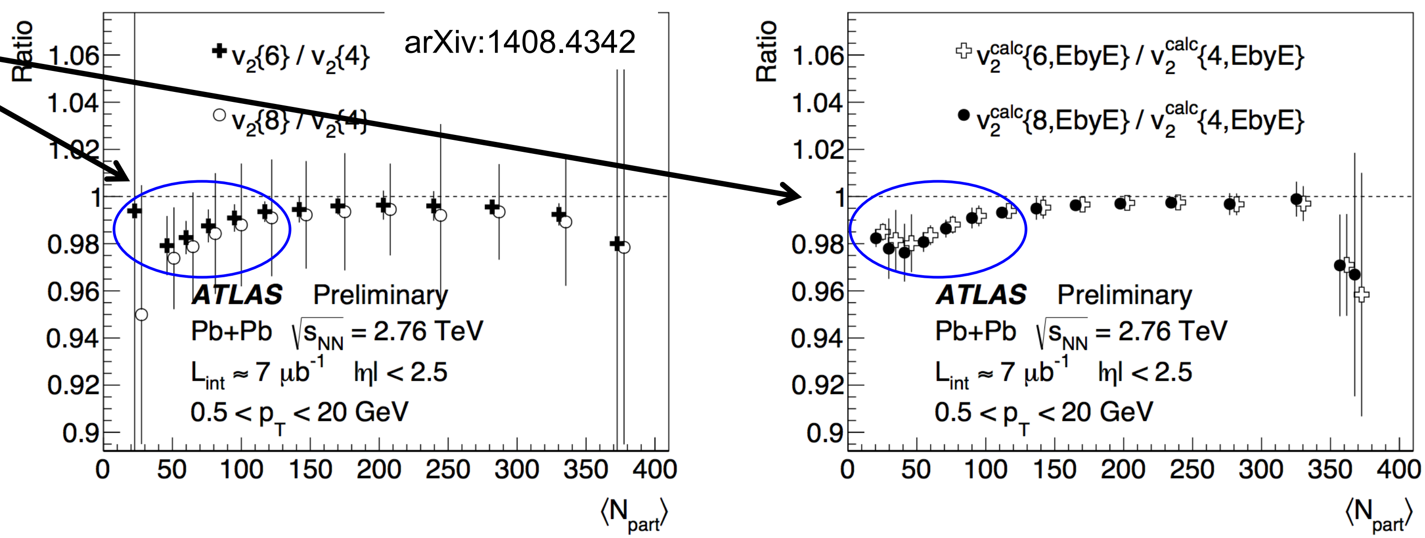

- Measuring $p(v_2)$ is equivalent to cumulants, more intuitive
- Non-Bessel Gaussian is reflected by a 2% change beyond 4^{th} order cumulants

More info by selecting on event-shape

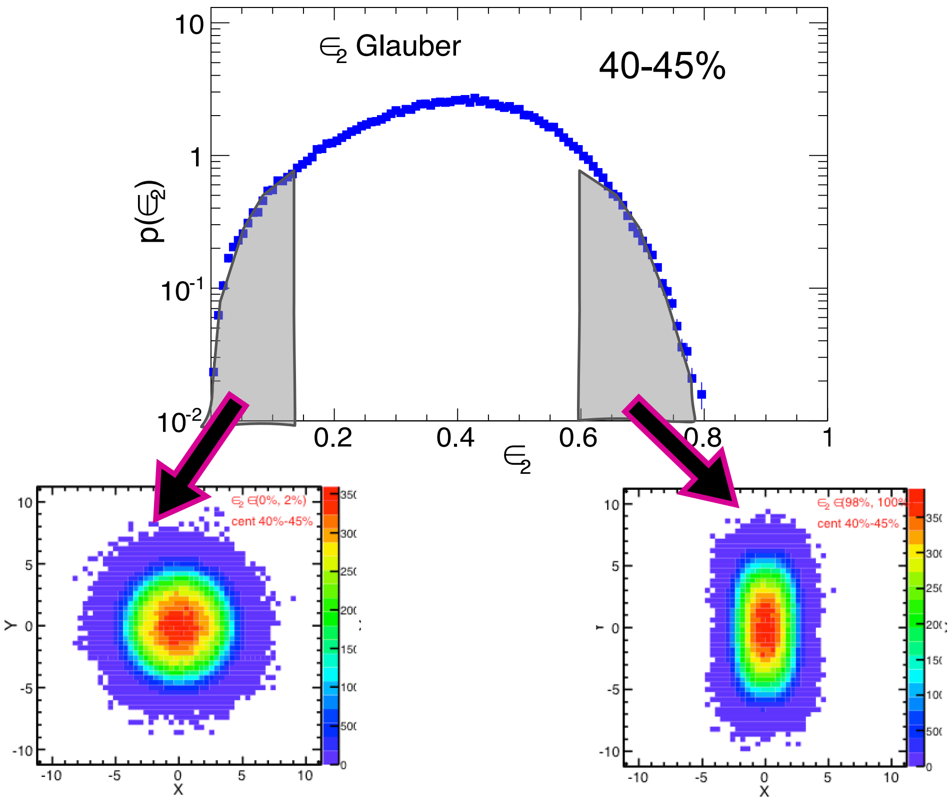

Jurgen, Anthony, Sergei
arXiv:1208.4563

Peng, Jiangyong, Soumya
arxiv:1311.7091

- Select events with certain v_2^{obs} in Forward Rapidity:

More info by selecting on event-shape

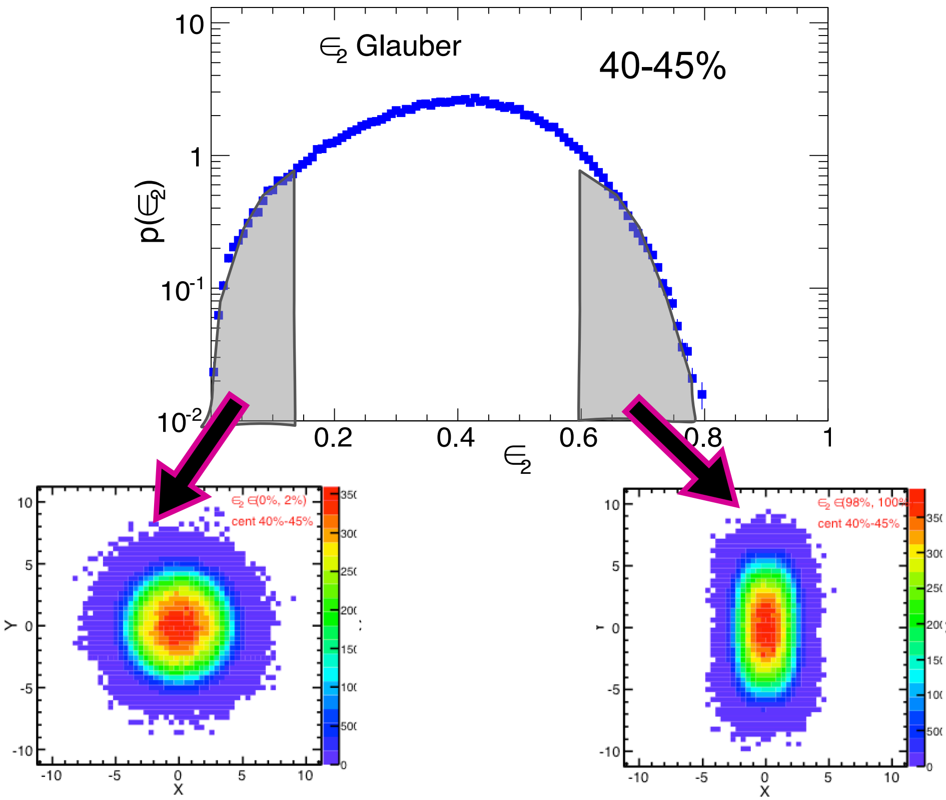

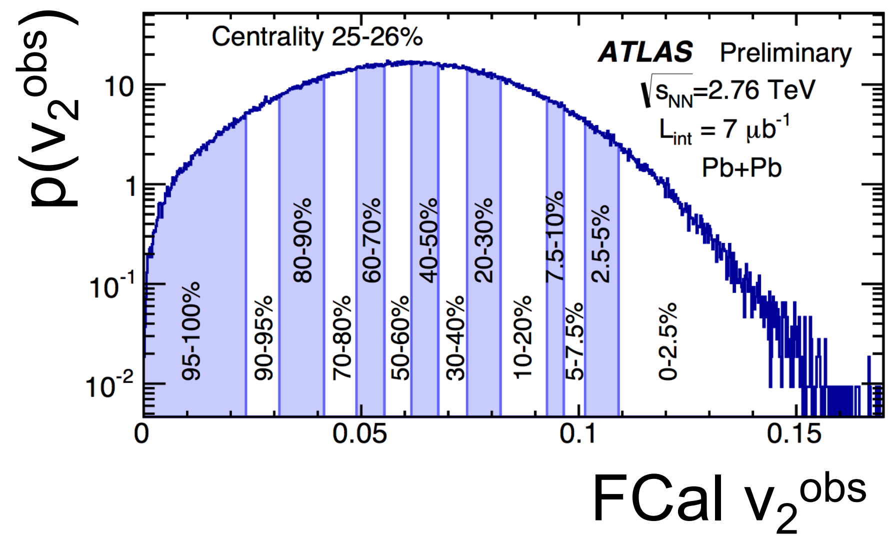

Jurgen, Anthony, Sergei
arXiv:1208.4563

Peng, Jiangyong, Soumya
arxiv:1311.7091

- Fix centrality, then select events with certain v_2^{obs} in Forward rapidity:

➔ATLAS: measure v_n via two-particle correlations in $|\eta|$< 2.5

Fix system size and change ellipticity!!

More info by selecting on event-shape

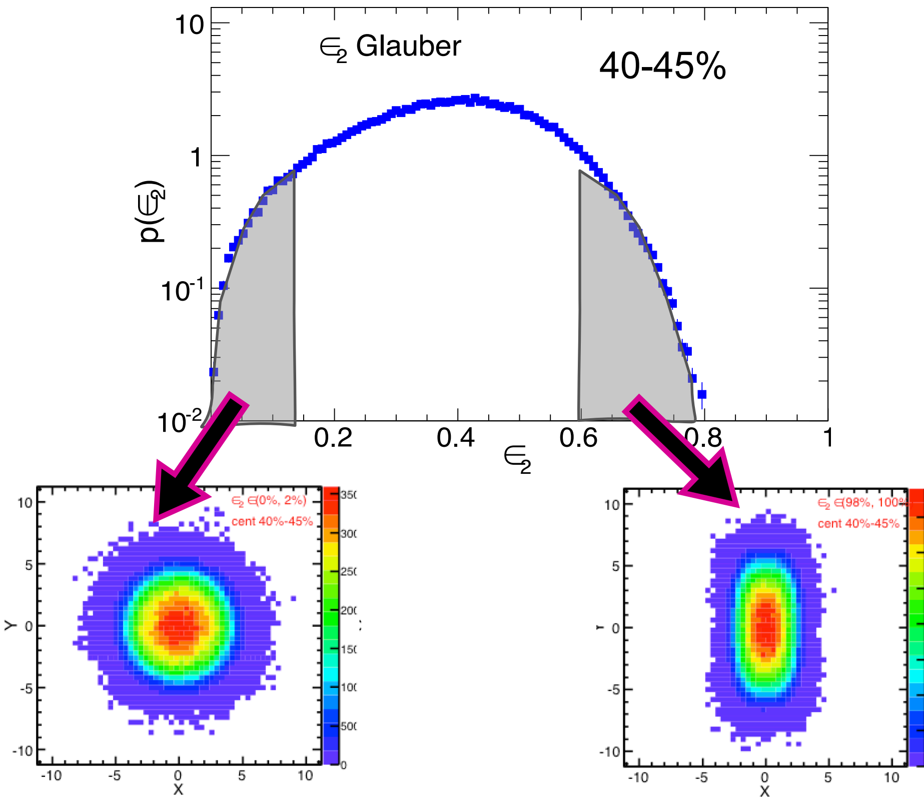

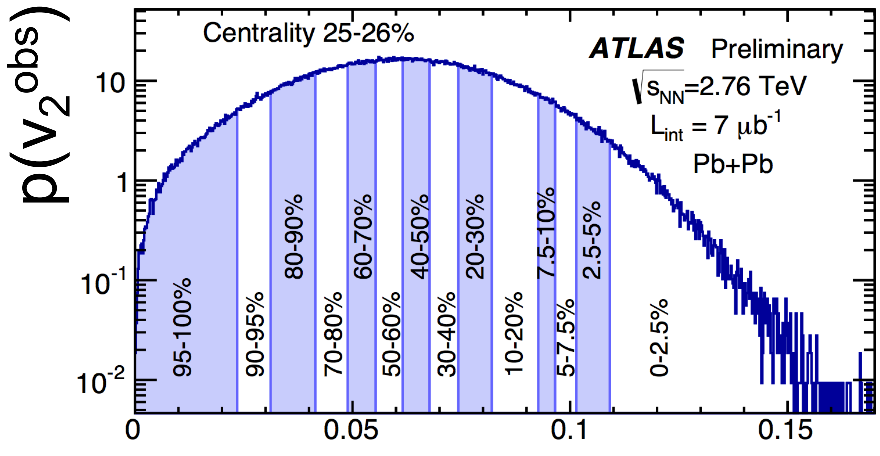

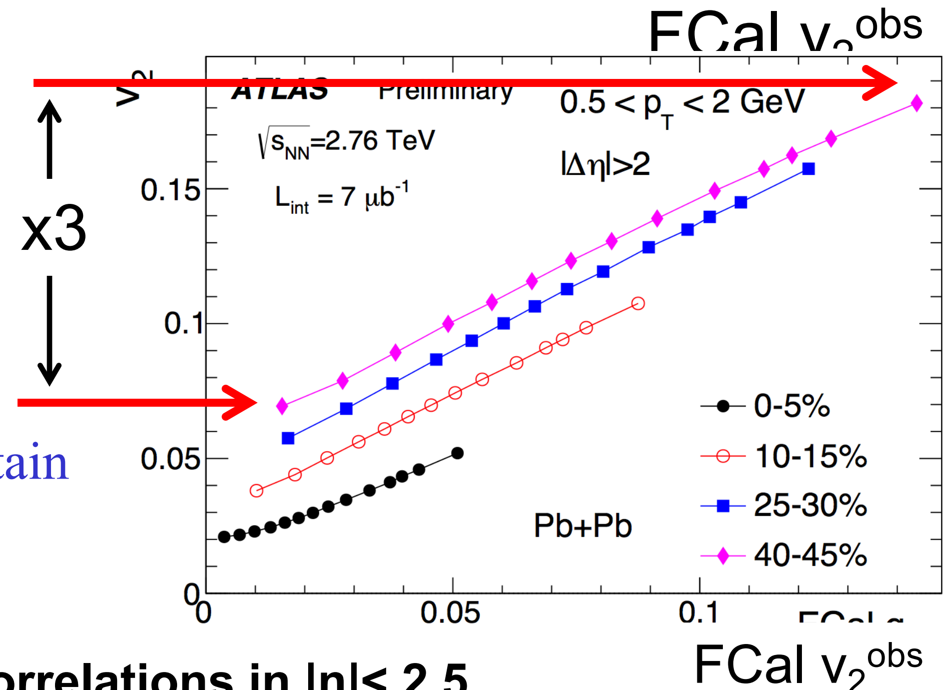

- Fix centrality, then select events with certain v_2^{obs} in Forward rapidity:

➔ATLAS: measure v_n via two-particle correlations in |η|< 2.5

Vary ellipticity by a factor of 3!

$p(v_n,v_m)$ via event-shape engineering tech.

- Directly observe the functional form (more info than symmetric cumulant)

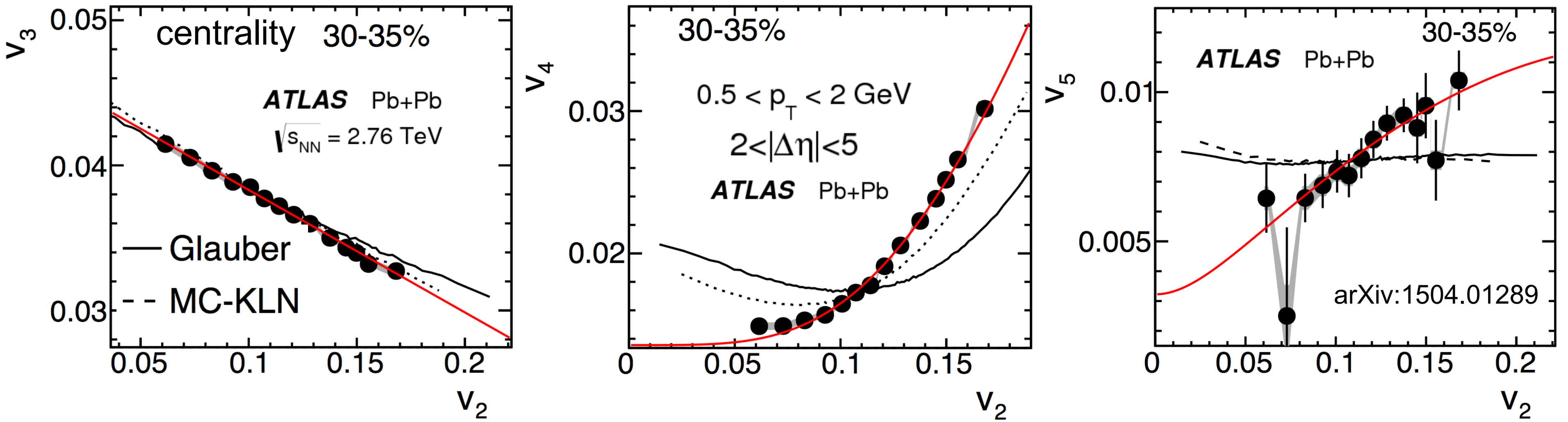

- Expected quadratic corr. for v_2-v_4, linear corr. for v_2-v_5 →final state mode-mixing

$$v_4 e^{i4\Psi_4} = c_0 e^{i4\Phi_4} + c_1 \left(v_2 e^{i2\Phi_2}\right)^2 \Rightarrow \text{ Fit by } v_4 = \sqrt{c_0^2 + c_1^2 v_2^4}$$

$$v_5 e^{i5\Psi_5} = c_0 e^{i5\Phi_5} + c_1 v_2 e^{i2\Phi_2} v_3 e^{i3\Phi_3} \Rightarrow \text{ Fit by } v_5 = \sqrt{c_0^2 + c_1^2 v_2^2 v_3^2}$$

- anti-correlation v_2-v_3 →anti-correlation of ε_2-ε_3 from initial state

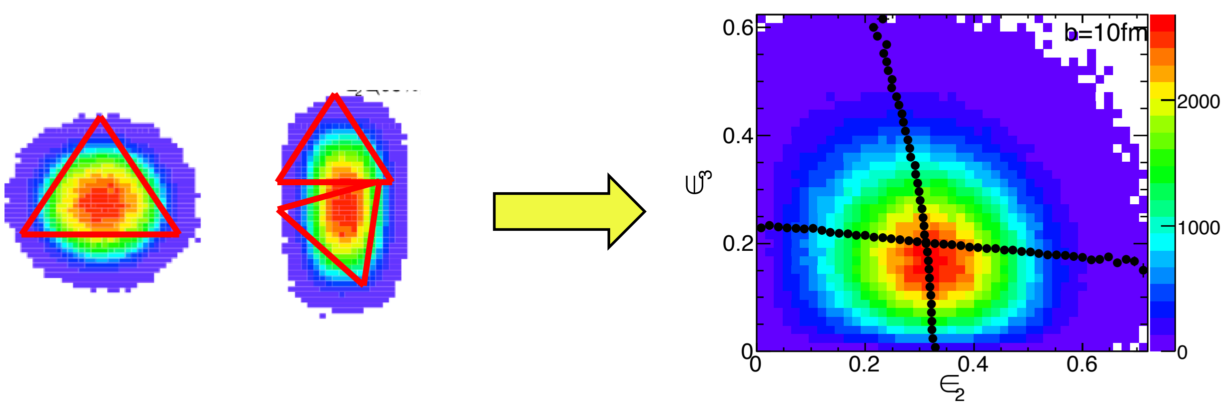

Longitudinal dynamics

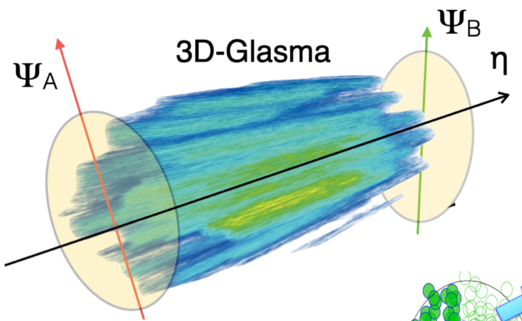

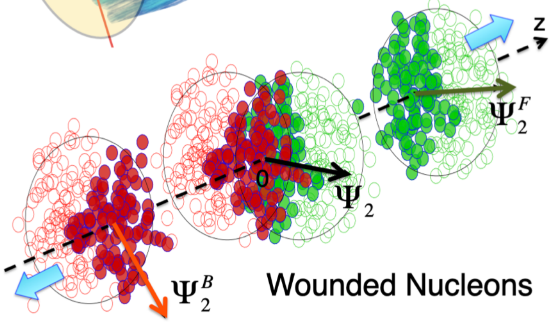

$$\boldsymbol{v}_n(\eta) = v_n(\eta)e^{in\Phi_n(\eta)}$$

$$\left\langle \vec{\varepsilon}_n(\boldsymbol{\eta}_1^s)\vec{\varepsilon}_n^{\,*}(\boldsymbol{\eta}_2^s)\right\rangle \Rightarrow \left\langle \vec{V}_n(\boldsymbol{\eta}_1)\vec{V}_n^{\,*}(\boldsymbol{\eta}_2)\right\rangle$$

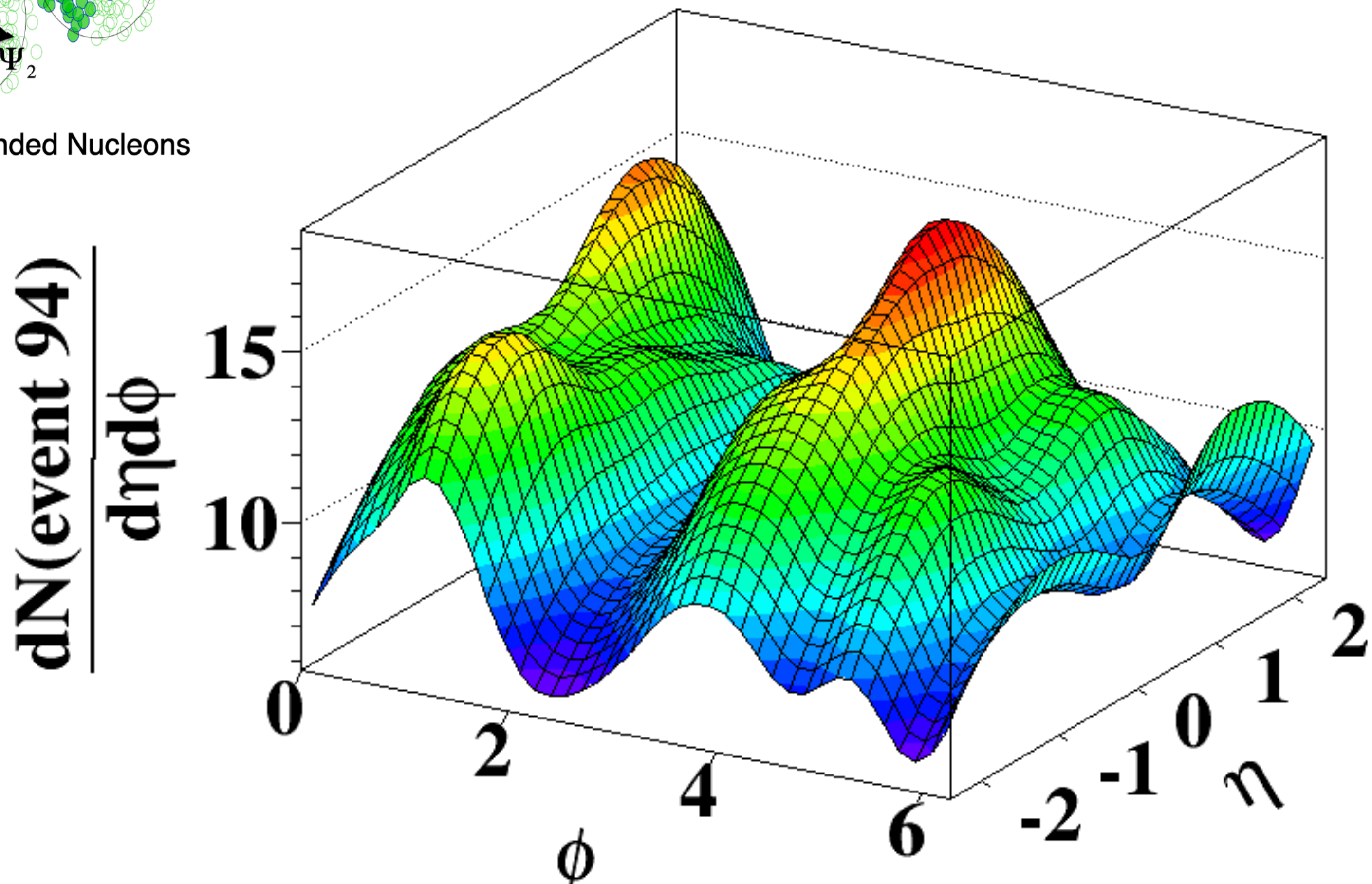

Curtsey of L.Pang and X.N Wang, EbyE 3D hydro+AMPT condition

Origin of flow decorrelation

Shape of overlap driven by eccentricity of F-going and B-going participants

$\varepsilon_n^F e^{in\Phi_n^F}$ $\varepsilon_n^B e^{in\Phi_n^B}$

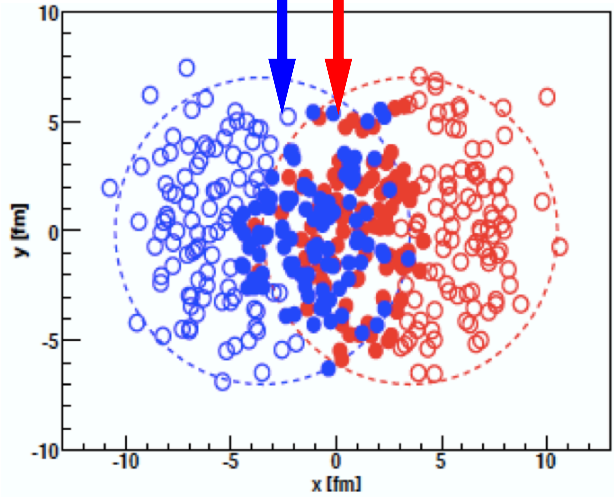

arXiv:1403.6077
arXiv:1402.6680

Consequence: $\boldsymbol{v}_n(\eta) = v_n(\eta) e^{in\Psi_n(\eta)}$ in a single event

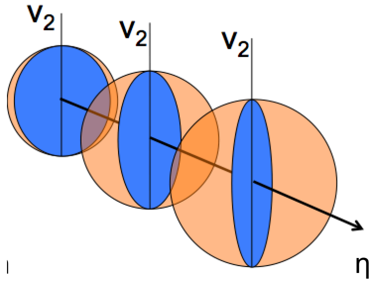

$v_n^F \neq v_n^B$

Asymmetry in flow magnitude

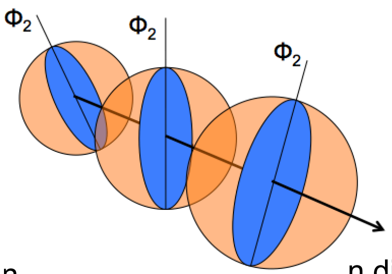

$\Psi_n^F \neq \Psi_n^B$

Torque/twist of flow plane

√s dependence of v_n decorrelation

CMS observable arXiv:1503.01692

arXiv:1709.02301,2001.04201

$$r_{n|n;1}(\eta)=\frac{V_{n\Delta}(-\eta,\eta_{ref})}{V_{n\Delta}(\eta,\eta_{ref})}$$

quantify the decorrelation between -η and η

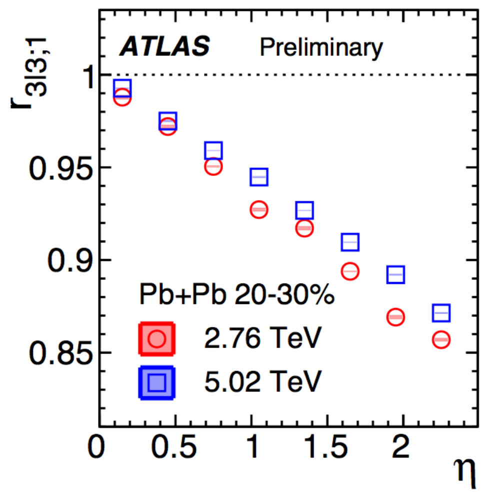

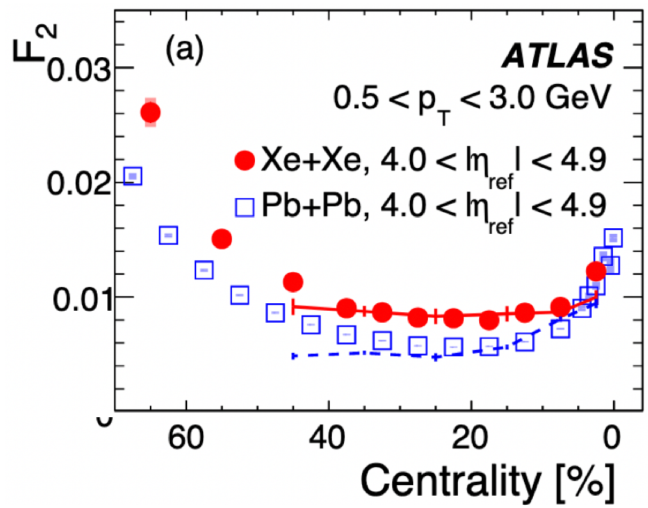

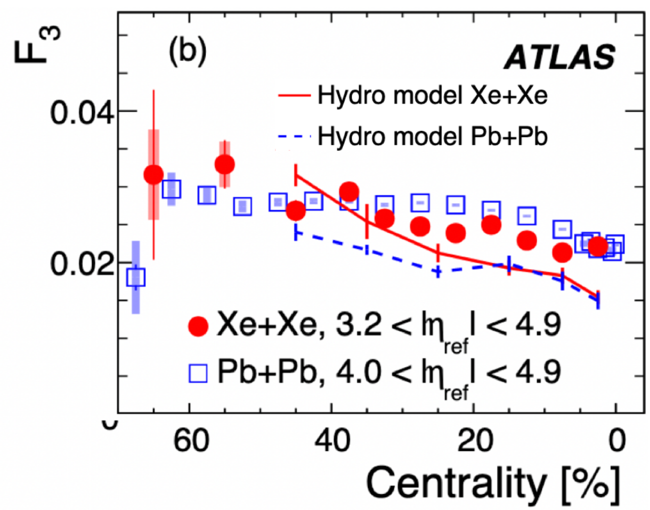

$$r_{n|n;1} = 1 - 2F^{r}_{n;1}\eta$$

Centrality dependence of F_n reflects geometry effects

√s dependence of v_n decorrelation

CMS observable arXiv:1503.01692

arXiv:1709.02301,2001.04201

$$r_{n|n;1}(\eta) = \frac{V_{n\Delta}(-\eta,\eta_{ref})}{V_{n\Delta}(\eta,\eta_{ref})}$$

quantify the decorrelation between -η and η

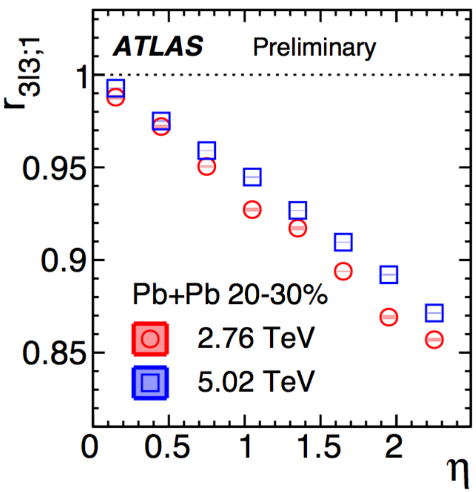

$$r_{n|n;1} = 1 - 2F^{r}_{n;1}\eta$$

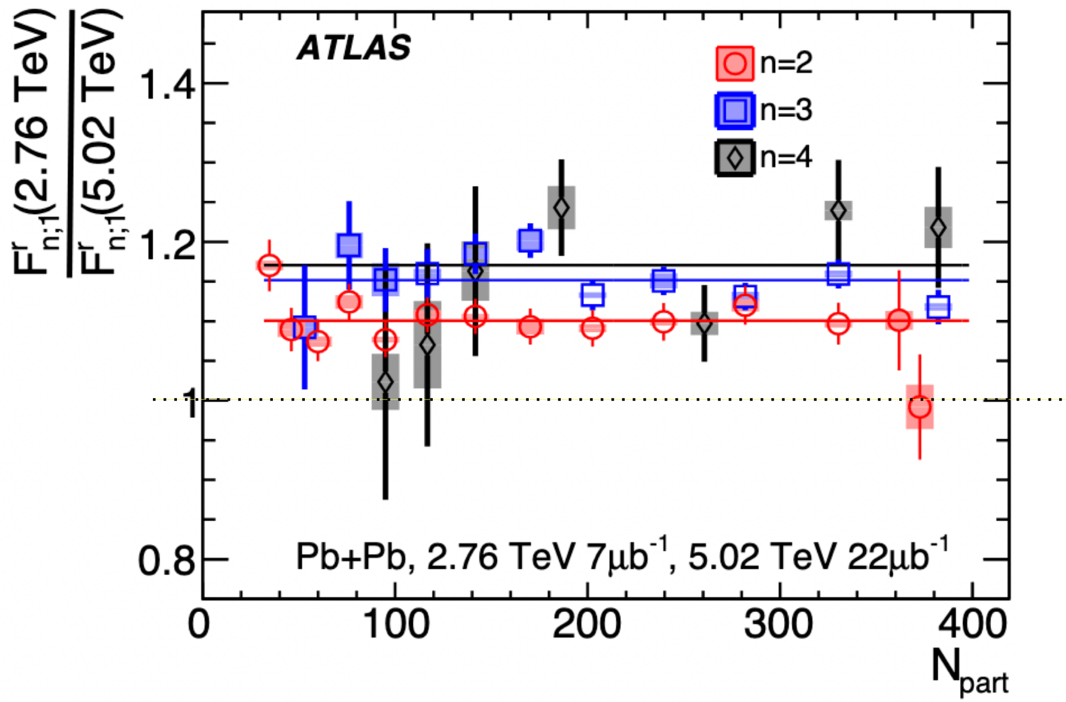

Centrality dependence of F_n reflects geometry effects

Decorrelation of v_2,v_3 & v_4 is 10-20% stronger in 2.76 TeV

$\sqrt{s}$ dependence of v_n decorrelation

CMS observable arXiv:1503.01692

$$r_{n|n;1}(\eta) = \frac{V_{n\Delta}(-\eta,\eta_{ref})}{V_{n\Delta}(\eta,\eta_{ref})}$$

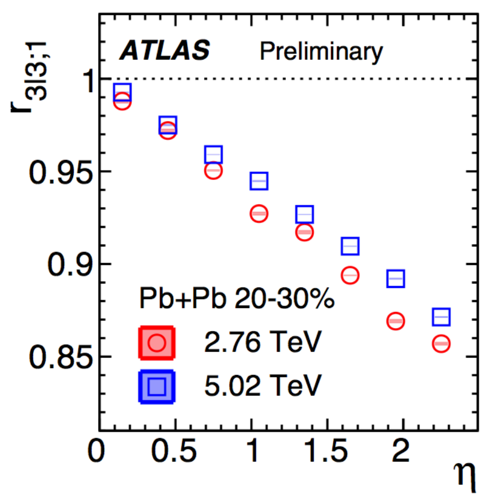

$$r_{n|n;1} = 1 - 2F^{r}_{n;1}\eta$$

arXiv:1709.02301,2001.04201

quantify the decorrelation between -η and η

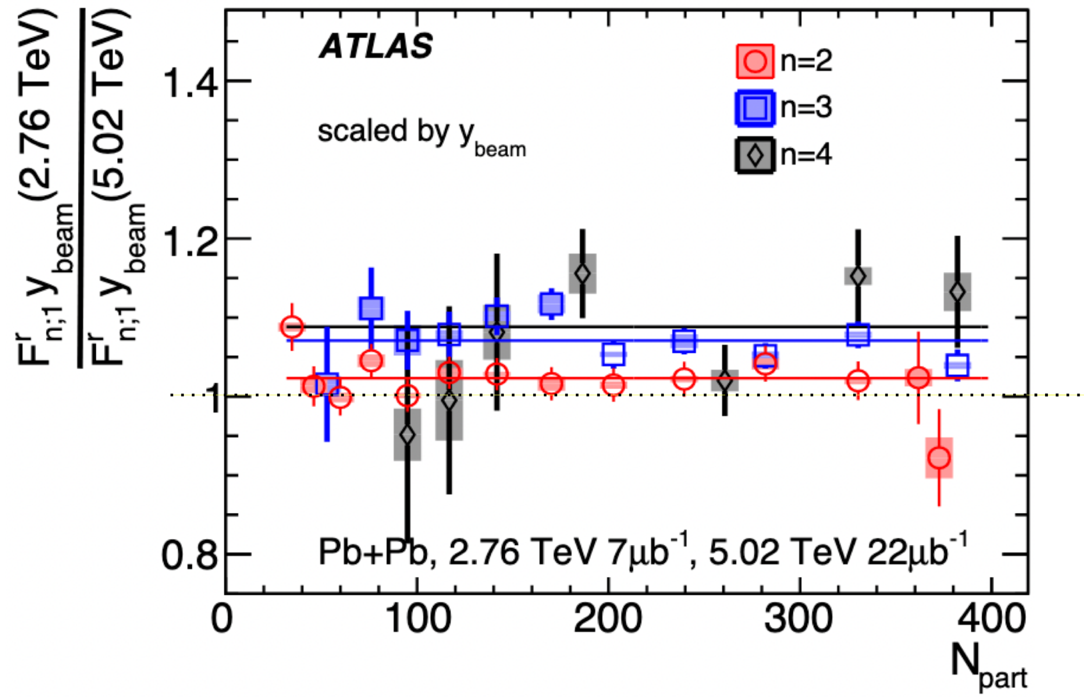

Centrality dependence of F_n reflects geometry effects

Decorrelation of v_2,v_3 & v_4 is 10-20% stronger in 2.76 TeV

Scale by beam rapidity removes most difference

$$F_n \propto 1/y_{\rm beam}$$
$$y_{\rm beam} = \ln(\sqrt{s_{\rm NN}}/2)$$

$$\Rightarrow \frac{F_n(2760\text{GeV})}{F_n(5020\text{GeV})} = \frac{y_{\rm beam}(5020\text{GeV})}{y_{\rm beam}(2760\text{GeV})} = 1.08$$

√s dependence of v_n decorrelation

CMS observable arXiv:1503.01692

arXiv:1709.02301,2001.04201

$$r_{n|n;1}(\eta) = \frac{V_{n\Delta}(-\eta,\eta_{ref})}{V_{n\Delta}(\eta,\eta_{ref})}$$

quantify the decorrelation between -η and η

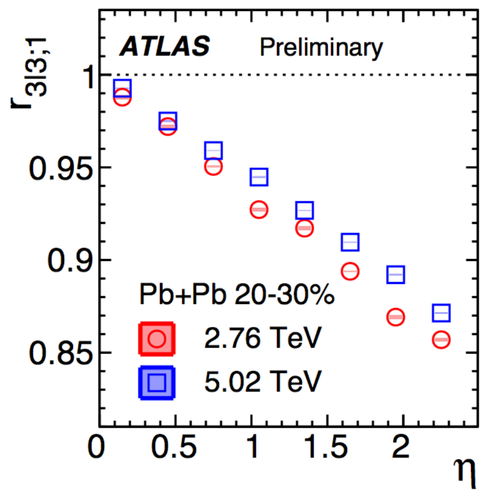

$$r_{n|n;1} = 1 - 2F^{r}_{n;1}\eta$$

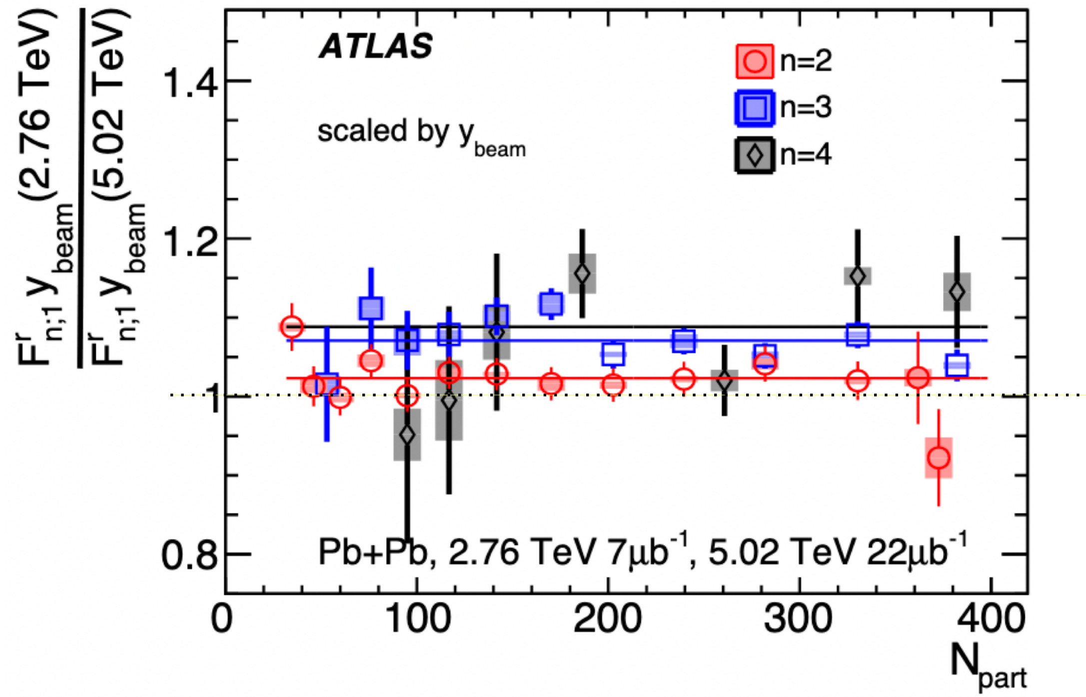

Extensive set of new observables also measured

- Higher-moments of longitudinal decorrelation
- Separating v_n asymmetry and event-plane twist
- Longitudinal decorrelation between v_n and v_m

System dependence: Xe+Xe vs PbPb

- Consider Glauber model with parameterized longitudinal structure
  - Describe v_n-ratio vs N_{part}→ viscous effects controls by overall size
  - Describe F_n-ratio vs $N_{part}/2A$→ control by overall shape not the size

arXiv: 1709.02301
arXiv: 2001.04201

- Better agreement than hydro→due to wrong longitudinal initial state?

Ratio of inclusive flow

$$\frac{v_n^{\mathrm{XeXe}}}{v_n^{\mathrm{PbPb}}} \approx \frac{\varepsilon_n^{\mathrm{XeXe}}}{\varepsilon_n^{\mathrm{PbPb}}}$$

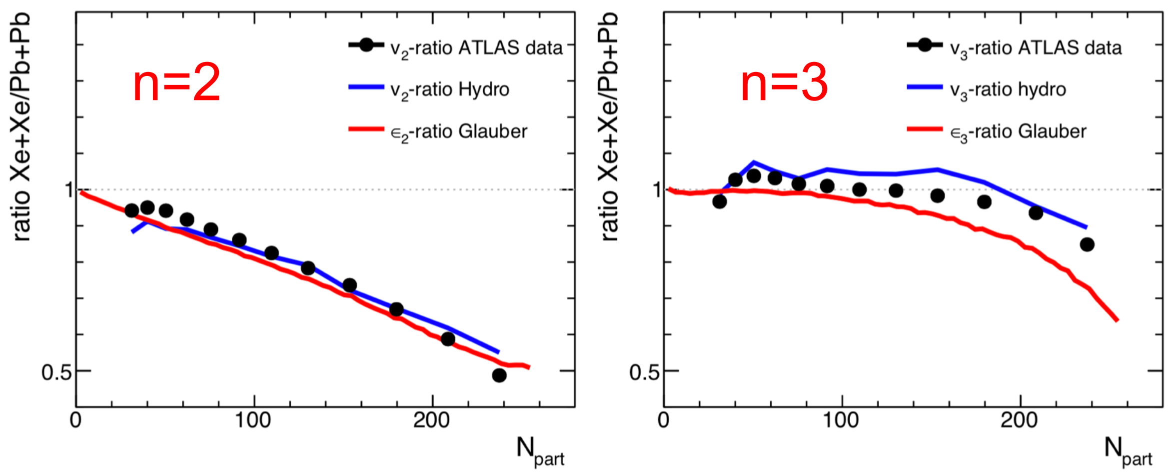

Ratio of flow decorrelation

$$r_n = 1 - 2F_n\eta$$

$$F_n \propto A_n = \frac{\langle(\mathcal{E}_n^{\mathrm{F}} - \mathcal{E}_n^{\mathrm{B}})^2\rangle}{\langle(\mathcal{E}_n^{\mathrm{F}} + \mathcal{E}_n^{\mathrm{B}})^2\rangle}$$

$$\frac{F_n^{\mathrm{XeXe}}}{F_n^{\mathrm{PbPb}}} \approx \frac{A_n^{\mathrm{XeXe}}}{A_n^{\mathrm{PbPb}}}$$

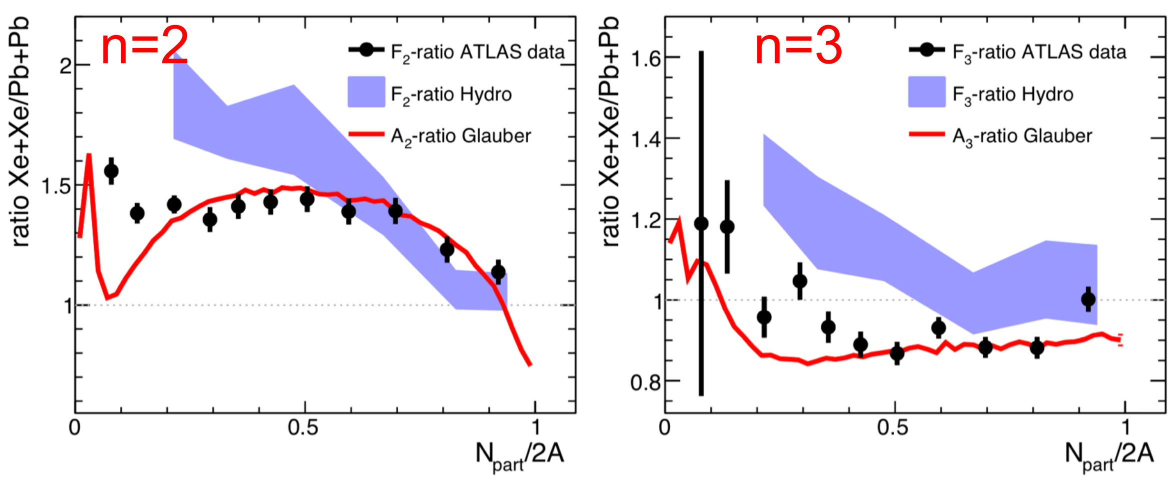

Outlook

Strategy: systematically peering into earlier time from large to smaller systems

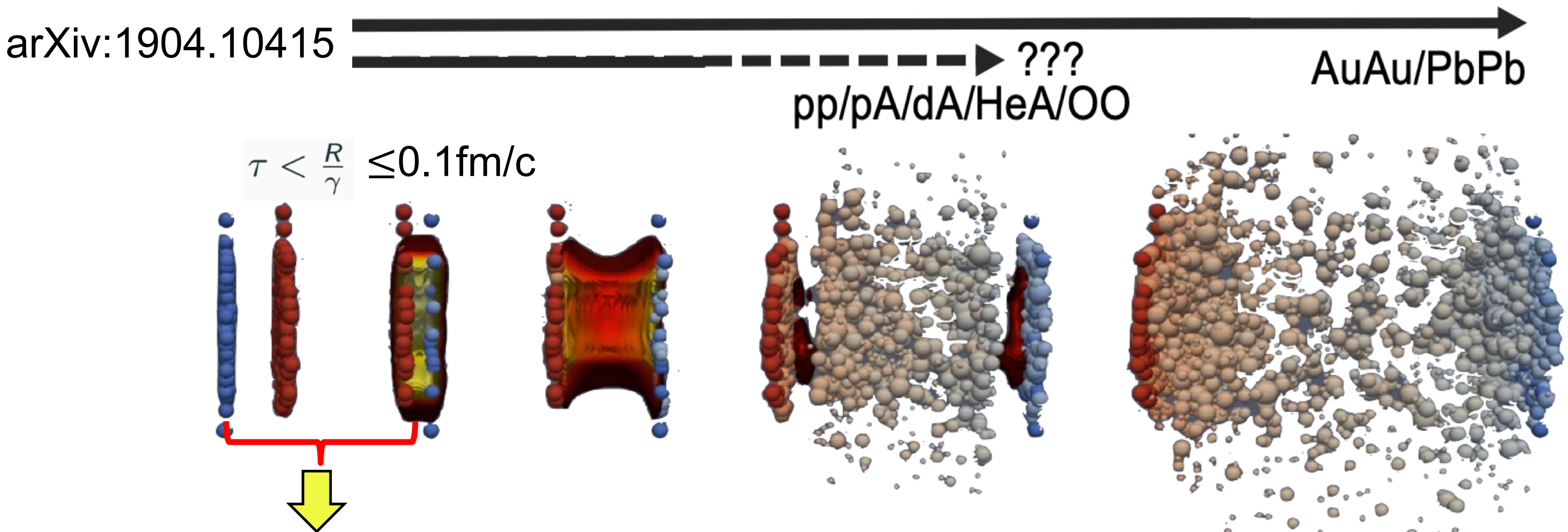

Goal: Quantify the initial condition and emergence of collectivity

Strategy: constrain initial condition “independently” with nuclear structure input

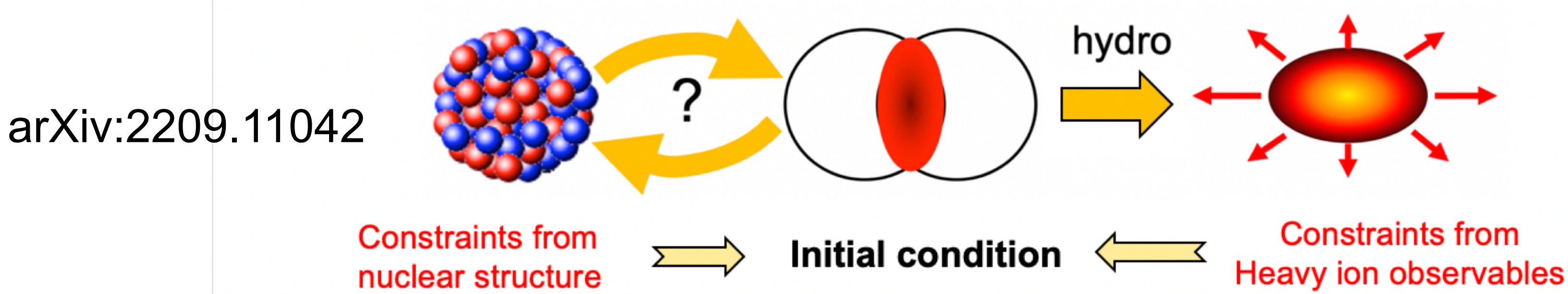

Intersection to nuclear structure: a new research frontier

https://indico.bnl.gov/event/13769/

Workshop Organizers

- Jiangyong Jia (Stony Brook)
- Chun Shen (RBRC/Wayne State)
- Derek Teaney (Stony Brook)
- Zhangbu Xu (BNL)

https://indico.gsi.de/event/14430/

ExtreMe Matter Institute EMMI

EMMI Rapid Reaction Task Force

Nuclear Physics Confronts Relativistic Collisions of Isobars

Heidelberg University, Germany, May 30 – June 3 & October 12-14 2022

Organizers:
Giuliano Giacalone
Jiangyong Jia
Vittorio Somà
You Zhou

https://esnt.cea.fr/Phocea/Page/index.php?id=107

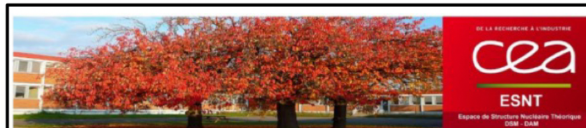

Deciphering nuclear phenomenology across energy scales

https://esnt.cea.fr/Phocea/Page/index.php?id=107 **Sep 20th - Sep 23rd 2022**

Organizers:
Giuliano Giacalone (ITP Heidelberg)
Jean-Yves Ollitrault (IPhT Saclay)
You Zhou (Niels Bohr Institute)

https://www.int.washington.edu/programs-and-workshops/23-1a

Intersection of nuclear structure and high-energy nuclear collisions

Organizers:
Jiangyong Jia (Stony Brook & BNL)
Giuliano Giacalone (ITP Heidelberg)
Jacquelyn Noronha-Hostler (Urbana-Champaign)
Dean Lee (Michigan State & FRIB)
Matt Luzum (São Paulo)
Fuqiang Wang (Purdue)

Jan 23rd - Feb 24th 2023

- Partonic structure of protons and nuclei
- Physics at low-x and gluon saturation
- The initial stages and nuclear structure in heavy-ion collisions
- Collective dynamics from small to large systems
- New theoretical techniques at large and small coupling
- New facilities: DIS and hadronic experiments

Do not let your imagination being limited by your detector!